

Material Matters™

Vol. 3, No. 4



Alternative Energy Generation and Storage



Alternative Energy—the way to go

Light-Driven
Generation of Hydrogen

Polymer Electrolyte
Membrane Fuel Cells

Polymer-based Materials
for Printed Electronics

Advanced
Lithium Ion Batteries

Introduction

Welcome to the fourth issue of **Material Matters™** for 2008, focused on 'Alternative Energy'.

Alternative energy may be broadly defined as energy generated in a way that does not deplete natural resources or harm the environment. It is used as an "alternative" to fossil fuels and other non-renewable energy sources such as coal, oil and natural gas. It is common knowledge that the use of fossil fuels contributes to global warming through the emission of carbon dioxide, and also pollutes the air, water, and soil. In addition, fossil energy sources are not sustainable, i.e. while global energy demand continues to grow, the world reserves of coal, oil and natural gas are being depleted. Currently, the world energy consumption has exceeded 400 quadrillion BTUs (4.2×10^{20} J) per year. The United States alone uses about one-quarter of the energy produced in the world, with an additional 29% consumed by the European Union, Japan and S. Korea. Every day, the USA needs 20 million barrels of oil, 60 billion cubic feet of natural gas, and 3 million tons of coal to cover its existing energy demand.

One of the ways currently being explored to satisfy growing energy requirements is the conversion of solar energy into electricity. This energy can be immediately used to power a broad variety of tools and devices. It can also be stored in chemical form in hydrogen rich chemical substances such as hydrides, or through the use of lithium ion batteries. The former approach—conversion of solar energy into materials with high hydrogen content such as oil and natural gas—is the way in which fossil fuels formed in nature to begin with; of course that process took millions of years.

This issue of **Material Matters** features four articles that are concerned with different aspects of alternative energy. Researchers at Penn State University highlight conversion of solar energy and water into hydrogen, using a biologically inspired electrochemical process. Hydrogen produced in such a manner could later be used in PEM fuel cells to generate electricity. Material issues in PEM fuel cells are the subject of the article by scientists from the US Department of Energy (US DOE) and the Argonne National Laboratory. Further ways to enable high efficiency solar power and lighting through photochemical generation of energy are discussed by researchers at Plextronics. Finally, scientists affiliated with the Vehicle Technologies Program of the US DOE address materials challenges in advanced lithium ion battery research.

Customary to **Material Matters**, each article in this issue is accompanied by Sigma-Aldrich® products helpful in the corresponding type of alternative energy research. The facing page lists the materials categories that you will find in this issue. Please visit Aldrich Materials Science at sigma-aldrich.com/matsci for product information. We invite you to send your comments and questions regarding **Material Matters** and materials of interest to matsci@sial.com.



Viktor Balema, Ph.D.
Materials Science
Sigma-Aldrich Corporation

About Our Cover

The energy of our own star – the sun, is abundant, free and virtually unlimited. Its conversion into electricity, which can be used directly or stored in batteries or energy-rich substances such as hydrogen, offers a perfect way to resolve a vast majority of current and future energy issues. The system that combines biologically inspired *Photosystem I*, a 1,6-hexanedithiol molecule shown on the cover, and either gold or platinum nanoparticles, represents one of the possible ways to capture and convert solar energy into hydrogen (see article on p. 78) for further use in fuel cells (see article on p. 85) to power homes, offices and a variety of electrical and electronic devices.

Material Matters™

Vol. 3 No. 4

Aldrich Chemical Co., Inc.
Sigma-Aldrich Corporation
6000 N. Teutonia Ave.
Milwaukee, WI 53209, USA

To Place Orders

Telephone 800-325-3010 (USA)
FAX 800-325-5052 (USA)

Customer & Technical Services

Customer Inquiries 800-325-3010
Technical Service 800-231-8327
SAFC® 800-244-1173
Custom Synthesis 800-244-1173
Flavors & Fragrances 800-227-4563
International 414-438-3850
24-Hour Emergency 414-438-3850
Web site sigma-aldrich.com
Email aldrich@sial.com

Subscriptions

To request your **FREE** subscription to **Material Matters**, please contact us by:

Phone: 800-325-3010 (USA)

Mail: **Attn: Marketing Communications**
Aldrich Chemical Co., Inc.
Sigma-Aldrich Corporation
P.O. Box 355
Milwaukee, WI 53201-9358

Website: sigma-aldrich.com/mm
Email: sams-usa@sial.com

International customers, please contact your local Sigma-Aldrich office. For worldwide contact information, please see back cover.

Material Matters is also available in PDF format on the Internet at sigma-aldrich.com/matsci.

Aldrich brand products are sold through Sigma-Aldrich, Inc. Sigma-Aldrich, Inc. warrants that its products conform to the information contained in this and other Sigma-Aldrich publications. Purchaser must determine the suitability of the product for its particular use. See reverse side of invoice or packing slip for additional terms and conditions of sale.

All prices are subject to change without notice.

Material Matters (ISSN 1933-9631) is a publication of Aldrich Chemical Co., Inc. Aldrich is a member of the Sigma-Aldrich Group. © 2008 Sigma-Aldrich Co.

"Your Materials Matter."



Joe Porwoll

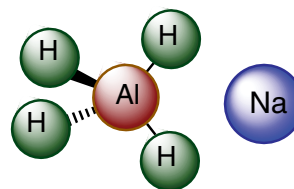
Joe Porwoll, President
Aldrich Chemical Co., Inc.

Do you have a compound that you wish Sigma-Aldrich® could list to help materials research? If it is needed to accelerate your research, it matters—please send your suggestion to matsci@sial.com and we will be happy to give it careful consideration.

Dr. Ragaiy Zidan of Savannah River National Laboratory kindly suggested that we offer a 1M solution of sodium aluminum hydride in tetrahydrofuran ($\text{NaAlH}_4/\text{THF}$ **Aldrich Prod. No. 698865**) as a material for alternative energy applications.¹ The solution of NaAlH_4 in THF is a base-material for advanced energy storage systems. Its electrolysis² creates aluminum hydride (AlH_3), with hydrogen content of 10% by weight and a hydrogen release temperature of $\sim 100^\circ\text{C}$. This enables the development of low-cost hydrogen storage systems with thermodynamics and kinetics meeting transportation requirements.³

References:

(1) Balema, V.P. *Material Matters* **2007**, vol 2, issue 2, 2. (2) Zidan, R. Electrochemical Reversible Formation of Alane. http://www.hydrogen.energy.gov/pdfs/review08/stp_19_zidan.pdf (accessed Oct 24, 2008). Patent application filed. (3) Read, C.; Thomas, G.; Ordaz, G.; Satyapal, S. *Material Matters* **2007**, vol 2, issue 2, 3.



Sodium aluminum hydride solution

[13770-96-2] NaAlH_4 FW 54.00

F: 10

► 1 M in tetrahydrofuran

density.....0.905 g/mL, 25 °C

698865-1L

1 L

Alternative Energy Products Featured in this Issue

Materials Category	Content	Page
Functionalized Nanoparticles	Gold and silver functionalized nanoparticles	82
Bifunctional Materials for Self-Assembled Monolayers (SAMs)	Dithiols, carboxylic acids and other bifunctional materials for SAMs	82
Selected Nanopowders for Energy Applications	Selected metal and metal oxide nanopowders for energy applications	83
Catalyst Materials for PEM Fuel Cells	Carbon supported, non-carbon supported and unsupported platinum group metals catalysts	88
Membrane Materials for PEM Fuel Cells	Membranes, solutions, dispersions and other membrane materials for fuel cell applications	89
Electrode Materials for Solid Oxide Fuel Cells (SOFC)	Anode and cathode materials for use in Solid Oxide Fuel Cells	90
Electrolyte Materials for Solid Oxide Fuel Cells (SOFC)	Oxide materials for use as electrolytes in Solid Oxide Fuel Cells	90
Organic Electronic Materials: Plexcore® Products	Electronic grade semi-conducting and conducting inks	96
Organic Photovoltaic Materials: Light-Emitters, Dopants and Electron Acceptors	Electron acceptors and sublimed grade organic light-emitters and dopants	97
Organic Photovoltaic Materials: Indium Tin Oxide/Indium Oxide	Indium Tin Oxide/Indium Oxide coated slides, PET Sheets and Indium Tin Oxide (ITO) powders	98
Select Materials for Battery Applications	Electrode materials, electrolyte materials and solvents for advanced Li-batteries	103

A Biologically-Inspired Electrochemical Half-Cell for Light-Driven Generation of Hydrogen



Rebecca A. Grimme¹ and John H. Golbeck*^{1,2}

¹Department of Chemistry, The Pennsylvania State University University Park, PA 16802

²Department of Biochemistry and Molecular Biology, The Pennsylvania State University, University Park, PA 16802

*E-mail: jhg5@psu.edu

Introduction

An economy based on hydrogen has long been touted as one of the most promising routes to a sustainable energy future. Hydrogen gas (H₂) is a particularly clean source of energy that can be utilized efficiently in hydrogen-based fuel cells. Because the product of energy conversion is H₂O, the use of H₂ does not exacerbate the already existing problem of CO₂ accumulation that is a major component of global climate change. Despite its desirable attributes, H₂ is not found in nature and methods must be employed to generate it using other sources of energy.

Commercial methods of producing hydrogen are expensive. These processes include electrolysis of water and steam reforming of methane. The generation of hydrogen from the electrolysis of water takes place in an electrolytic cell where an electrical power source is connected to a cathode and to an anode, each in separate vessels connected via a salt bridge. The negatively charged electrode combines electrons with protons, and this is where hydrogen is produced. The electrolysis of water requires a larger input of energy than would otherwise be necessary due to the fact that 100% of the electrical power put into the cell is not converted into the chemical bond energy of hydrogen.¹ Steam reforming of methane is less expensive than the electrolysis of water and is therefore the preferred industrial method of production. The heating of steam and methane to high temperatures in the presence of a nickel catalyst results in the generation of H₂ and CO. The further reaction of H₂O and CO produces additional H₂ and CO₂. The by-product of the reaction, CO₂, however, adds to the problem of climate change. Also, because energy is lost by the conversion of methane into hydrogen, it makes little sense to use one perfectly good fuel to generate another.

With all of the drawbacks associated with currently utilized methods of hydrogen production, researchers are increasingly looking to sunlight as a means of supplying the necessary energy input. Sunlight is abundant, widely distributed, and virtually inexhaustible. The amount of solar energy that strikes the surface of the earth in one hour is more than sufficient to satisfy the total global demand for energy in an entire year.² Hence, the photocatalytic production of hydrogen is emerging as an attractive route to the generation of a renewable source of fuel.

Emerging Technologies

A large amount of research has focused on the generation of H₂ by systems that employ gold (Au, **Aldrich Prod. No. 636347**) or platinum (Pt, **Aldrich Prod. No. 685453**) nanoparticles supported on semiconductor surfaces such as TiO₂ (**Aldrich Prod. Nos. 635057, 635049, 635065**). These semiconductor systems function by absorbing a photon and creating an electron-hole pair. The electron migrates to the Au or Pt nanoparticles that are located on the semiconductor surface. These nanoparticles catalyze hydrogen production. A major drawback to this type of system lies in the fact that the band gap of TiO₂ semiconductors is large, and photons with sufficient energy to generate the electron-hole pair can be found only in ultraviolet (UV) radiation.⁶ UV, which is light with wavelengths between 200 and 400 nm, constitutes only a small percentage of the solar radiation that reaches the surface of the earth. In an attempt to overcome the band-gap limitation, organic dyes can be introduced into these semiconductor systems to increase the absorption of solar radiation.³⁻⁵ These dyes absorb photons in the visible portion of solar radiation and are thus able to inject electrons into the conduction band of the semiconductor materials.^{4,5} Once electrons are in the conduction band, they migrate to the Au or Pt nanoparticles loaded on the surface, thereby enabling hydrogen production. While these dye sensitized systems increase the functional working wavelengths that are capable of sustaining the charge-separated state necessary for hydrogen production, organic dyes are degraded by illumination and moisture, limiting the usefulness of these devices.

Biological and Biohybrid Systems for Light Driven Hydrogen Production

While the dye-sensitized and semiconductor-supported nanoparticle systems hold promise, newer investigations have focused on using both biological systems and biohybrid designs to photocatalytically generate H₂. It is generally accepted that any photocatalytic system for generating a usable fuel from sunlight will require three components: a module that converts sunlight into an electric current, a module that catalyzes the reduction of protons to H₂, and a linker that facilitates the transfer of electrons from the light module to the catalytic module.

One such system couples Photosystem I (PS I), a naturally occurring light harvesting complex, to hydrogen evolving catalysts. The advantages of utilizing PS I as the energy-converting module are discussed in detail below. *In vivo* experiments using photosynthetic organisms have shown that hydrogen can be evolved by the enzymes nitrogenase (N₂ase) and hydrogenase (H₂ase).^{7,8} Hydrogen is produced as a byproduct of nitrogen fixation by N₂ase and it is a natural product of H₂ase when an electron donor is present.⁷ When the reducing equivalents from PS I are directed to H₂ases or N₂ases (the linker being a redox protein), cyanobacteria and microalgae evolve hydrogen.⁸ A major drawback to these *in vivo* systems is that the efficiency of hydrogen generation will always be limited due to the amount of solar energy necessary to sustain the growth and metabolism of the organism. A further drawback is that N₂ases and H₂ases are oxygen sensitive, making hydrogen generation problematic in the presence of oxygenic photosynthesis.

In vitro systems that combine biological and/or non-biological components in novel ways were the first attempt at a hybrid approach for hydrogen production. These *in vitro* systems utilize isolated proteins or proteins within chloroplasts in conjunction with metal deposition and/or naturally occurring H_2 ases. A PS I- H_2 ase construct has been created by fusing the gene encoding for the [NiFe]- H_2 ase from *Ralstonia eutropha* H16 with the gene encoding the PsaE (PS I stromal) protein. When the H_2 ase/PsaE fusion product is re-bound to a PsaE deletion mutant of PS I, hydrogen is evolved, albeit at low rates ($0.2 \mu\text{mol } H_2 \text{ mg Chl}^{-1} \text{ h}^{-1}$).⁹ Greenbaum and coworkers have pioneered the use of PS I/metal nanoparticle constructs for the photocatalysis of H_2 . In this work, Pt and other metals have been directly photoprecipitated on the stromal side of both isolated PS I proteins and PS I contained within spinach chloroplasts.^{10,11} Illumination of these platinized chloroplasts and PS I proteins enables the production of H_2 , but again at low rates of 0.2 to $2.0 \mu\text{mol } H_2 \text{ mg Chl}^{-1} \text{ h}^{-1}$. In a more recent study, the cross-linking of the naturally-occurring electron donor plastocyanin was shown to double the rates of hydrogen production achieved from platinized PS I.¹²

Efficient Photon Capture and Energy Conversion by PS I

PS I is a light harvesting complex that is located in the photosynthetic membranes of plants and cyanobacteria, a photosynthetically active bacteria. The major purpose of PS I is to use the energy of light to transfer electrons from high potential (i.e. low energy) redox proteins across the membrane to low potential (i.e. high energy) redox proteins.¹³

Figure 1 depicts the arrangement of PS I proteins within the membrane. Although PS I comprises 13 proteins, only PsaA, PsaB, and PsaC are of interest for this article. PsaA and PsaB are intramembrane proteins which support the core electron transfer cofactors of PS I, while PsaC lies outside of the membrane and acts as an interface to shuttle electrons from within the membrane to soluble low potential electron accepting proteins. **Figure 2** affords a more detailed look at the organization of PS I. Additional intramembrane proteins surround the PsaA/PsaB heterodimer and support ~100 antenna chlorophyll molecules that are active in light harvesting.¹⁴ These antenna pigments in cyanobacterial PS I are chlorophyll *a* (Chl *a*) molecules that are capable of absorbing photons with wavelengths shorter than 700 nm. This absorbance corresponds to 43-46% of the total solar radiation that reaches the surface of the earth.¹⁵ When a Chl *a* molecule absorbs a photon, an excited state is created; the energy is ultimately transferred by resonance energy transfer to the primary electron donor of PS I, a Chl *a* special pair, termed P700. The arrangement of the core electron transfer cofactors is shown in **Figure 3**. When the exciton reaches P700, a charge-separated state occurs between P700 and the primary electron acceptor, A_0 , another Chl *a* molecule. Ultimately, the electron is transferred through the other electron transfer cofactors to F_B , the terminal cofactor within PS I. The F_B cluster has a midpoint potential of -580 mV , which is more than sufficient to reduce protons to H_2 .¹³ The quantum yield of PS I approaches 1.0 which means that nearly all of the photons that PS I absorbs are converted to the charge separated state $P700^+/F_B^-$.

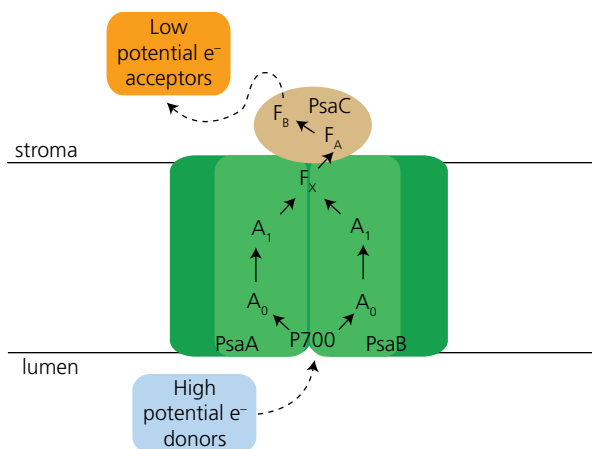


Figure 1. This cartoon depicts Photosystem I within the thylakoid membrane. PsaA and PsaB (light green) are an intramembrane protein heterodimer that contain the core electron transfer cofactors within PS I—P700, A_0 , A_1 , and F_x . PsaC lays outside of the membrane on the stromal side of PS I and harbors the electron transfer cofactors F_x and F_B . Additional intramembrane proteins (dark green) support antenna chlorophyll molecules that are responsible for light harvesting. High potential (low energy) electron donating proteins (plastocyanin or cytochrome c_6) provide electrons to P700. The light-driven electron transfer through the membrane is photocatalyzed by photons absorbed by the antenna chlorophyll molecules. Electrons ultimately arrive on the stromal side of PS I at F_B and can then transfer to soluble low potential (high energy) electron accepting proteins (ferredoxin or flavodoxin).

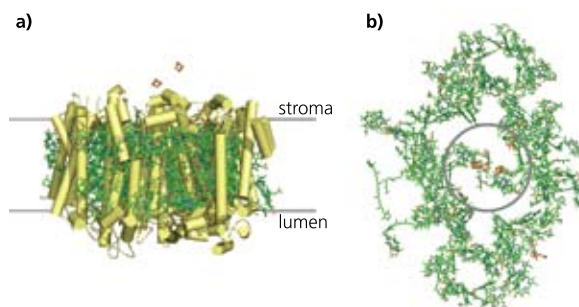


Figure 2. a) The intramembrane α -helices of PS I (yellow tubes) act as scaffolds for antenna Chl *a* molecules (green) and the core electron transfer cofactors; the [4Fe-4S] clusters, F_x and F_B , are visible on the stromal side. b) Rotating structure (a) 180° and removing the protein scaffold affords a look (top down from the stromal side) at the organization of the antenna Chl *a* molecules around the core electron transfer cofactors (circled in grey).

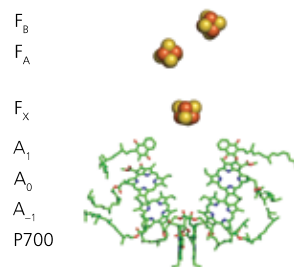


Figure 3. The core electron transfer cofactors are arranged to allow for light-induced electron transfer to occur rapidly from P700, through the cofactors, to F_B . A charge-separated state is first established between P700 and A_0 . The electron is then transferred to A_1 , a bound phyloquinone molecule, and then to three [4Fe-4S] clusters. The first of these, the inter-polypeptide [4Fe-4S] cluster, F_x , is ligated by cysteine residues provided by both PsaA and PsaB. The stromal protein PsaC harbors the two terminal [4Fe-4S] clusters, F_A and F_B .

Electron transfer on the PS I acceptor side is thermodynamically favorable, as the midpoint potential of each of the subsequent cofactors is more positive than the previous one. **Figure 4** shows the potentials of the electron transfer cofactors as a function of their distance from P700 as well as forward electron transfer and charge-recombination times. The electron transfer from P700 to F_B is rapid (~ 200 ns) and the lifetime of the charge-separated state, $P700^+/F_B^-$, is long (~ 65 ms).¹⁶ Provided the electron is transferred away from the F_B cluster within this lifetime, charge recombination will not occur and electron can be harnessed for useful work. In the case of normal photosynthesis, this work is the reduction of ferredoxin or flavodoxin (and the subsequent production of NADPH), but if the electron can be removed at F_B^- directly, it can be used to reduce protons to H_2 .

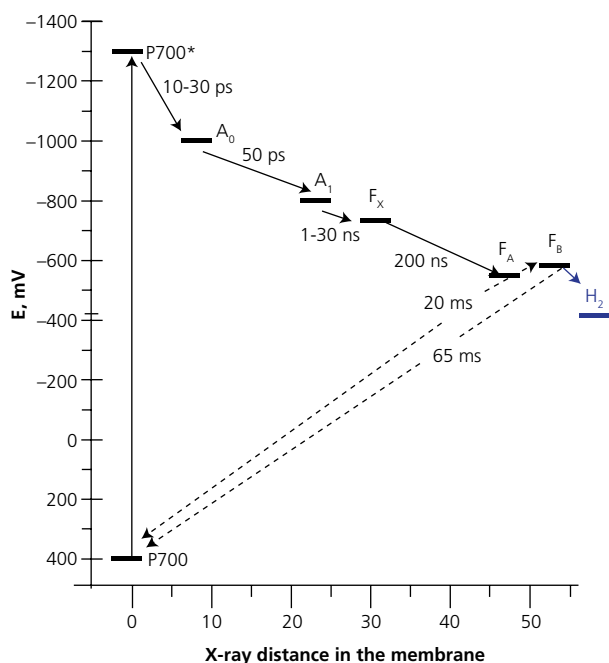


Figure 4. As the electron is transferred away from P700, the potential of the cofactors becomes more positive, thus the transfer is thermodynamically downhill and favorable. Further electron transfer from F_B^- to a H_2 evolving entity (Pt nanoparticle or H_2 ase enzyme) is also thermodynamically favorable as the redox potential for H_2 evolution is thermodynamically more positive than that of the F_B cluster.

Hydrogen Catalysis by Pt Nanoparticles

As in the case of semiconductor systems, Pt nanoparticles can be used as the catalyst for hydrogen generation. H^+ ions adsorb onto the Pt surface and combine with an electron to form an H atom. A covalent bond is catalytically generated between two adsorbed H atoms to yield H_2 . H_2 then desorbs from the Pt surface. At pH 7.0, this process occurs at a midpoint potential of -420 mV. If the electrons are derived from the F_B cluster of PS I, there is ~ 160 mV of thermodynamic driving force for this reaction to occur. This translates to an equilibrium constant $>10^2$, indicating that this reaction will be a highly favorable reaction on thermodynamic grounds.

In practice, a system could be set up in which PS I and Pt nanoparticles are suspended in solution, however hydrogen generation would most likely be of low yield due to the fact that the interactions between nanoparticles and PS I would be controlled by slow diffusion chemistry. The speed of diffusion decreases as size of the body in motion increases. In this case, both the PS I and the Pt nanoparticles are large entities and diffusion would likely be too slow to transfer the electron from F_B^- to the nanoparticle surface before the charge recombination between $P700^+$ and F_B^- would occur. In order to avoid this inevitable loss of energy, a direct link should be made between the PS I and the Pt nanoparticle.

Molecular Wires Form a Covalent Pathway

Molecular wires are the answer to the diffusional limitation in electron transfer. A molecular wire, in the form of an aliphatic or aromatic hydrocarbon chain, can be used to connect PS I with the Pt nanoparticle. On one hand, the molecular wire should be sufficiently long to shield the protein from the nanoparticle surface to limit protein denaturation. On the other hand, the molecular wire should be sufficiently short enough to allow for efficient energy transfer between the two modules. Because the charge-separated state $P700^+/F_B^-$ is stable for ~ 65 ms, efficient electron transfer away from F_B must occur on the order of 1 ms. Marcus theory, which relates the rate of electron transfer to the distance between the cofactors (as well as the Gibbs free energy change, reorganization energy, and temperature), governs the maximum distance between PS I and the Pt nanoparticle for optimal electron transfer. Under ideal conditions, for the electron to be transferred on the microsecond timescale, the distance between the cofactors should be shorter than 2.0 nm. Short aliphatic and aromatic hydrocarbons with thiol moieties easily functionalize Pt nanoparticle surfaces and are commercially available (See product table 'Functionalized Nanoparticles' on pg 82). Unfortunately, a direct bond cannot be made to native PS I without modification.

Manipulation of PS I

In order to attach the molecular wire, a variant of the PsaC subunit must be engineered in which the native cysteine ligand to the F_B cluster is replaced with a glycine residue. Glycine lacks a side chain, and is hence incapable of ligating the Fe atom. However, its use opens up a site to which a molecular wire can be attached. The iron-free form of the PsaC variant is expressed in *Escherichia coli* and the F_A and F_B clusters are inserted using inorganic [4Fe-4S] clusters ligated by 2-mercaptoethanol (**Sigma Prod. No. M7522**). The PsaC variant can then be re-bound to previously-prepared PS I cores that lack the PsaC subunit. Analytical techniques show that two [4Fe-4S] clusters are inserted into the protein despite the absence of one of the cysteine ligands to F_B . This anomaly has been explained by the fact that the [4Fe-4S] clusters are inserted into the protein *in vitro* by a ligand exchange mechanism in which the 2-mercaptoethanol ligands are displaced by the protein cysteine ligands. At the glycine position, the 2-mercaptoethanol is retained, where it functions as a

so-called rescue ligand for the F_b cluster. The insertion process, incidentally, is driven to completion by the entropic gain realized when seven 2-mercaptoethanol molecules are released into solution during the insertion process. Thiol functionalities in the form of a molecular wire can then readily displace the single 2-mercaptoethanol ligand through facile sulfur-iron displacement reactions.^{17,18}

Catalytic Hydrogen Production Using Bioconjugates

Bioconjugates composed of rebuilt PS I containing the glycine variant of PsaC, 1,6-hexanedithiol (**Aldrich Prod. No. H12005**) molecular wires, and 3 nm Pt nanoparticles are assembled as shown in **Figure 5**. Sodium ascorbate (**Sigma Prod. No. A7631**) serves as the sacrificial electron donor to dichlorophenylindophenol (DCPIP) (**Sigma-Aldrich Prod. No. 119814**), which donates electrons directly to P700⁺. When the module is illuminated, H₂ is generated at a rate of 9.6 $\mu\text{mol H}_2 \text{ mg Chl}^{-1} \text{ h}^{-1}$ (0.23 mol H₂ mol PS I⁻¹ s⁻¹) over a period of 24 hr. The addition of cytochrome c₆, which is a superior electron donor to P700⁺, results in hydrogen generation at a rate of 49.3 $\mu\text{mol H}_2 \text{ mg Chl}^{-1} \text{ h}^{-1}$ (1.17 mol H₂ mol PS I⁻¹ s⁻¹).¹⁹

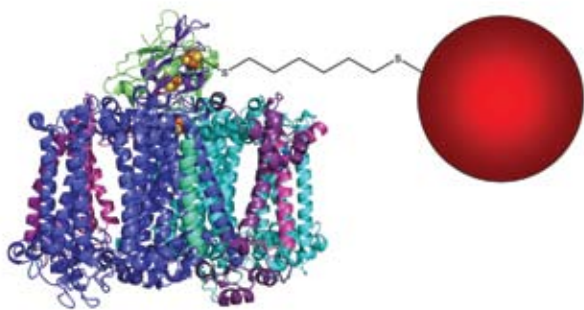


Figure 5. This bioconjugate is composed of Photosystem I rebuilt from recombinantly expressed C13G/C33S variant PsaC, PsaD, and P700/F_x cores, a 1,6-hexanedithiol (**Aldrich Prod. No. H12005**) molecular wire, and either Au or Pt nanoparticles. The molecular wire serves not only as a covalent link between PS I and the nanoparticle but also acts as a conduit for electron transfer. The electron donor, cytochrome c₆, is not depicted here.

While the initial rates for this system were already promising, continued research has yielded better performance. Altering the pH and the ionic strength of the solution, changing the length and the aromaticity of the molecular wire, as well as cross-linking cytochrome c₆ to the rebuilt PS I promises to increase the rate of hydrogen generation by the PS I/molecular wire/Pt nanoparticle bioconjugate. The best rates of H₂ generation to-date are at pH 7.0 in 10 mM MgCl₂ and 10 mM NaCl using chemically-cross linked cytochrome c₆.

Summary

The ability to photocatalytically generate clean hydrogen fuel has the potential to satisfy the global demand for storable energy and has advantages over the costly and environmentally unfriendly current means of hydrogen production. Biologically inspired systems that employ PS I as a means of photon capture and as a source of reducing electrons are yielding promising results when attached to Pt nanoparticles for the light-driven generation of hydrogen.

References:

- (1) Rosen, M.A., Scott, D.S., *Int. J. Hydrogen Energy*, **1998**, *23*, 653.
- (2) United Nations Development Program, *World Energy Assessment Report: Energy and the Challenge of Sustainability*, **2003**, United Nations, New York.
- (3) Mizukoshi, Y., Makise, Y., Shuto, T., Hu, J., Tominaga, A., Shironita, S., Tanabe, S., *Ultrasonics Sonochem.*, **2007**, *14*, 387.
- (4) Gurusathan, K., Maruthamuthu, P., Sastri, M.V.C., *Int. J. Hydrogen Energy*, **1997**, *22*, 57.
- (5) Dhanalakshmi, K.B., Latha, S., Anandan, S., Maruthamuthu, P., *Int. J. Hydrogen Energy*, **2001**, *26*, 669.
- (6) Tang, H., Berger, H., Schmid, P.E., Levy, F., *Solid State Commun.*, **1994**, *92*, 267.
- (7) Melis, A., Zhang, L., Forestier, M., Ghirardi, M.L., Seibert, M., *Plant Physiol.*, **2000**, *122*, 515.
- (8) Schutz, K., Happe, T., Troshina, O., Lindblad, P., Leitao, E., Oliveira, P., Tamagnini, P., *Planta*, **2004**, *218*, 350.
- (9) Ihara, M., Nishihara, H., Yoon, K.S., Lenz, O., Friedrich, B., Nakamoto, H., Kojima, K., Honma, D., Kamachi, T., Okura, I., *Photochem. Photobiol.*, **2006**, *82*, 676.
- (10) Lee, J.W., Tevault, C.V., Blankinship, S.L., Collins, R.T., Greenbaum, E., *Energy & Fuels*, **1994**, *8*, 770.
- (11) Millsaps, J.F., Bruce, B.D., Lee, J.W., Greenbaum, E., *Photochem. Photobiol.*, **2001**, *73*, 630.
- (12) Evans, B.R., O'Neill, H.M., Hutchens, S.A., Bruce, B.D., Greenbaum, E., *Nano Lett.*, **2004**, *10*, 1815.
- (13) Brettel, K., *Biochim. Biophys. Acta*, **1997**, *1318*, 322.
- (14) Jordan, P., Fromme, P., Witt, H.T., Klukas, O., Saenger, W., Krauss, N., *Nature*, **2001**, *411*, 909.
- (15) Gibbs, M., Holoander, A., Kok, B., Krampitz, L.O., San Pietro, A., A report on a workshop held September 5-6, 1973, at Bethesda, MD, supported by NSF under RANN Grant GI 40253 to Indiana University.
- (16) Shinkarev, V.P., Vassiliev, I.R., Golbeck, J.H., *Biophys. J.*, **2000**, *78*, 363.
- (17) Antonkine, M.L., Maes, E.M., Czernuszewicz, R.S., Breitenstein, C., Bill, E., Falzone, C.J., Balasubramanian, R., Lubner, C.E., Bryant, D.A., Golbeck, J.H., *Biochim. Biophys. Acta*, **2007**, *1767*, 712.
- (18) Que, L. Jr., Bobrik, M.A., Ibers, J.A., Holm, R.H., *J. Am. Chem. Soc.*, **1974**, *96*, 4168.
- (19) Grimme, R.A., Lubner, C.E., Bryant, D.A., Golbeck, J.H., *J. Am. Chem. Soc.*, **2008**, *130*, 6308.

Gold and Silver Functionalized Nanoparticles

Name	Structure	Concentration	Particle Size	Cat. No.
Octanethiol functionalized gold nanoparticles		2 % (w/v) in toluene	2 - 4 nm (DLS)	660426-5ML
Dodecanethiol functionalized gold nanoparticles		2 % (w/v) in toluene	2 - 4 nm (DLS)	660434-5ML
(1-Mercaptoundec-11-yl)tetra(ethylene glycol) functionalized gold nanoparticles		2 % (w/v) in H ₂ O	3.5 - 5.5 nm (TEM)	687863-5ML
1-Mercapto-(triethylene glycol) methyl ether functionalized gold nanoparticles		2 % (w/v) in absolute ethanol	3.5 - 5.5 nm (TEM)	694169-5ML
Decanethiol functionalized silver nanoparticles		0.1 % (w/v) in hexane	3 - 7 nm (DLS)	673633-25ML
Dodecanethiol functionalized silver nanoparticles		0.25 % (w/v) in hexane	5 - 15 nm (DLS)	667838-25ML

Bifunctional Materials for Self-Assembled Mono-Layers

For a complete list of self-assembly materials please visit sigma-aldrich.com/selfassembly.

Name	Structure	Purity	Cat. No.
4-Cyano-1-butanethiol		97%	692581-500MG
Biphenyl-4,4'-dithiol		95%	673099-1G
4,4'-Dimercaptostilbene		>96%	701696-100MG
2,2'-(Ethylenedioxy)diethanethiol		95%	465178-100ML 465178-500ML
6-Mercaptohexanoic acid		90%	674974-1G
8-Mercaptooctanoic acid		95%	675075-1G
3-Mercapto-1-propanol		95%	405736-1G 405736-5G
6-Mercapto-1-hexanol		97%	451088-5ML 451088-25ML
9-Mercapto-1-nonanol		96%	698768-1G
1,6-Hexanedithiol		96%	H12005-5G H12005-25G
1,8-Octanedithiol		≥97%	O3605-1G O3605-5G
NanoThinks™ THIO8		-	662615-100ML
1,9-Nonanedithiol		95%	N29805-5G N29805-25G
p-Terphenyl-4,4''-dithiol		-	704709-100MG
p-Terphenyl-4,4''-dicarboxylic acid		-	704717-100MG

Selected Nanopowders for Energy Applications

For a complete list of nanopowder please visit sigma-aldrich.com/nano.

Name	Particle Size	Surface Area	Purity/Concentration	Cat. No.
Silver	<150 nm	-	99% trace metals basis	484059-5G
Silver	<100 nm	surface area 5.0 m ² /g	99.5% trace metals basis	576832-5G
Silver, dispersion	<100 nm (TEM)	-	10 wt. % in ethylene glycol	658804-5G 658804-25G
Silver, dispersion	~157 nm	-	0.25 mM in H ₂ O	675318-5ML
Gold	<100 nm	-	99.9+% trace metals basis	636347-1G
Platinum	<50 nm (BET)	-	99.9+%	685453-500MG
Titanium(IV) oxide, mixture of rutile and anatase	<100 nm (BET) <50 nm (XRD)	spec. surface 15 m ² /g	99.9% trace metals basis	634662-25G 634662-100G
Titanium(IV) oxide, mixture of rutile and anatase	~21 nm (average particle size of starting nanopowder) <250 nm (DLS)	BET surf. area 50(±18) m ² /g (BET surface area of starting nanopowder)	99.9% trace metals basis, 53-57 wt. % in diethylene glycol monobutyl ether/ethylene glycol	700355-25G
Titanium(IV) oxide, mixture of rutile and anatase	<150 nm (DLS) ~21 nm (average particle size of starting nanopowder)	-	99.9% trace metals basis, 33-37 wt. % in H ₂ O	700347-25G 700347-100G
Titanium(IV) oxide, mixture of rutile and anatase	~15 nm <150 nm (DLS)	BET surf. area 102 m ² /g (BET surface area of starting nanopowder)	99.9% trace metals basis, 43-47 wt. % in xylene	700339-100G
Titanium(IV) oxide, anatase	<25 nm	spec. surface 200-220 m ² /g	99.7% trace metals basis	637254-50G 637254-100G 637254-500G
Titanium(IV) oxide, rutile	<100 nm	spec. surface 130-190 m ² /g	99.5% trace metals basis	637262-25G 637262-100G 637262-500G
Zinc oxide	<100 nm	surface area 15-25 m ² /g	-	544906-10G 544906-50G
Zinc oxide	<50 nm (BET)	>10.8 m ² /g	>97%	677450-5G



Aldrich® Materials Science Catalog

Your Materials Matter

With over 4,000 products for:

- Alternative Energy
- Metal and Ceramic Science
- Micro/Nano Electronics
- Nanomaterials
- Organic Electronics and Photonics
- Polymer Science
- Books & Labware



To reserve your free copy, visit sigma-aldrich.com/mscatalogm

sigma-aldrich.com
SIGMA-ALDRICH®

Hydrogen Storage Materials: New Additions

Storing hydrogen in solids—hydrides, organic or inorganic materials, and metal-organic frameworks—offers a unique opportunity for its convenient and safe use in a broad variety of fuel cell applications. Aldrich's products for hydrogen storage are designed to satisfy the basic requirements for materials research. Information provided with our products includes purity, hydrogen content, impurity profiles and x-ray powder differentiation dots.

For our complete product offer please visit sigma-aldrich.com/hydrogen

Organic Hydrogen Storage Media & Linkers for Metal Organic Frameworks (MOFs)

Product Name	Prod. No.
1,3,5-Tris(4-carboxyphenyl)benzene ≥98%, ≤20 wt. % solvent	686859
Hexadecahydropyrene 95%	691704
4,4'-Bipiperidine	705845
Tetradecahydro-4,7-phenanthroline	705853

Hydrogen Storage Alloys

Product Name	Prod. No.
Zirconium-Iron alloy	693812
Zirconium-Scandium-Iron alloy	693804
Lanthanum-Nickel alloy	685933
Lanthanum-Nickel-Cobalt alloy	685968
Mischmetal-Nickel alloy	685976
Titanium-Manganese alloy TiMn ₂ , alloy 5800	685941
Hydrides	
Borane-ammonia complex 97%	682098
Calcium borohydride	695254
Lithium borodeuteride ≥95%	685917
Magnesium hydride hydrogen-storage grade	683043

Materials Issues in Polymer Electrolyte Membrane Fuel Cells



Nancy L. Garland*¹, Thomas G. Benjamin² and John P. Kopasz²

¹U.S. Department of Energy, 1000 Independence Avenue, S.W., Washington, D.C. 20585-0121

²Argonne National Laboratory, 9700 South Cass Avenue, Lemont, IL 60439

*E-mail: Nancy.Garland@ee.doe.gov

Introduction

Fuel cells have the potential to reduce the nation's energy use through increased energy conversion efficiency and dependence on imported petroleum by the use of hydrogen from renewable resources. The US DOE Fuel Cell subprogram emphasizes polymer electrolyte membrane (PEM) fuel cells as replacements for internal combustion engines in light-duty vehicles to support the goal of reducing oil use in the transportation sector. PEM fuel cells are the focus for light-duty vehicles because they are capable of rapid start-up, demonstrate high operating efficiency, and can operate at low temperatures.

The program also supports fuel cells for stationary power, portable power, and auxiliary power applications where earlier market entry would assist in the development of a fuel cell manufacturing and supplier base. The technical focus is on developing materials and components that enable fuel cells to achieve the fuel cell subprogram objectives, primarily related to system cost and durability.

For transportation applications, the performance and cost of a fuel cell vehicle must be comparable or superior to today's gasoline vehicles to achieve widespread penetration into the market and achieve the desired reduction in petroleum consumption. By translating vehicle performance requirements into fuel cell system needs, DOE has defined technical targets for 2010 and 2015. These targets are based on competitiveness with current internal combustion engine vehicles in terms of vehicle performance and cost, while providing improvements in efficiency of a factor of 2.5 to 3. The overall system targets are: a 60% peak-efficient, durable, direct hydrogen fuel cell power system for transportation at a cost of \$45/kW by 2010 and \$30/kW by 2015.

DOE's approach to achieving these technical and cost targets is to improve existing materials and to identify and qualify new materials.

Fuel Cell Description

A fuel cell electrocatalytically generates electricity in a manner analogous to batteries. However, in a fuel cell the electrodes are not consumed. Rather, a fuel cell consumes fuel (hydrogen for PEM fuel cells) at the anode and oxygen from the air at the cathode.

A catalyst is utilized at the anode to promote separation of the hydrogen's protons and electrons. The protons travel through a membrane material to the cathode while the electrons travel via an external circuit to the cathode where they combine with the protons and oxygen on the cathode catalyst to form water and complete the cycle. The combination of the anode/membrane/cathode layers is called the membrane electrode assembly (MEA).

To complete a cell, the MEA is usually sandwiched between gas diffusion layers and gas flow fields that distribute reactants to the electrodes and collect the current from the reaction. Each cell generates less than a volt so many cells are "stacked" in series to generate voltage at useful levels.

Current PEM Fuel Cell Materials

Conventional anodes and cathodes are comprised of small platinum (Pt) catalyst particles (2-5 nm) supported on porous carbon (**Aldrich Prod. No. 205923**) as shown in **Figure 1**.^{1,2} Such electrodes face a number of issues including Pt particle stability, especially under automotive duty cycles; carbon support corrosion; and insufficient catalytic activity to meet Pt content targets.

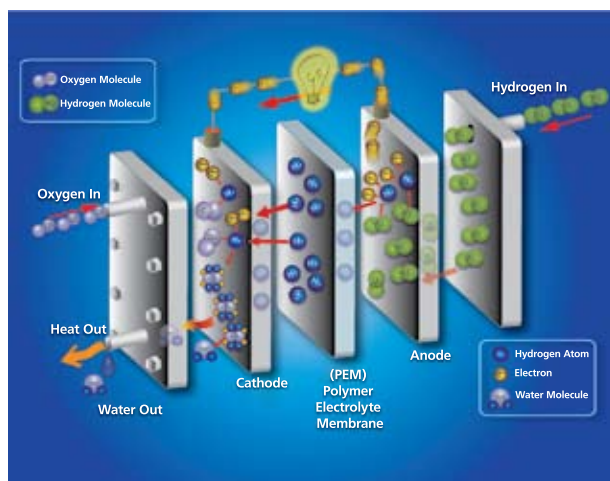


Figure 1. Illustration of polymer electrolyte membrane fuel cell operating on hydrogen fuel and oxygen from air.

Most of the current research on catalysts for PEM fuel cells is focused on the cathode. The general objectives are: to reduce Pt content (and thereby cost); to obtain higher catalytic activity than the standard carbon-supported platinum catalysts; and to increase the durability of the catalyst/support system, especially during transients and shutdown/startup cycles.³

The state-of-the-art membrane material is based on perfluorosulfonic acid that depends on the presence of water in the membrane to conduct the protons. The primary deficits of this material are: loss of conductivity at temperatures above 100°C and low humidity; insufficient conductivity at low temperature (-20°C); insufficient mechanical integrity; during humidity cycles which cause swelling and shrinking; and chemical stability. Most DOE membrane research is focused on durability and operation at temperatures above 100°C. Both mechanical and chemical durability are being addressed by physical reinforcement and by changes to the ionomer chemistry and structure and its end groups, respectively.

Fuel Cell Targets

To help achieve the high-level goals mentioned above and to guide component researchers, DOE has also developed targets for individual PEM fuel cell components. Targets for the electrocatalyst, membrane, and membrane electrode assembly are shown in Tables 1, 2, and 3, respectively. Successful validation of an advanced component requires that all targets be met simultaneously. A complete set of DOE's PEM fuel cell system, stack and component-level technical and cost targets are found in the DOE Office of Energy Efficiency and Renewable Energy Hydrogen, Fuel Cells & Infrastructure Technologies Program Multi-Year Research, Development and Demonstration Plan.⁴

Table 1 contains DOE targets specifically for the electrocatalyst and support. The key targets are related to cost (Pt content) and durability with cycling. For a service life of 5,000 hours (~150,000 miles) that is acceptable to consumers, automotive service is estimated to involve about 17,000 shutdown/startup cycles, 1,650 freeze cycles, and 1,200,000 load cycles.⁵

The 17,000 shutdown/startup cycles are particularly important because the anode, which is normally filled with hydrogen, can experience intrusion of air (oxygen) during shutdown. This results in mixed potentials at the anode and high potentials at the cathode, causing highly corrosive conditions.³

Depending on the severity of the 1,200,000 load (voltage) cycles during vehicle operation, the Pt on the electrodes can dissolve and redeposit, causing changes in Pt particle morphology and a loss of performance.

Table 1. Electrocatalyst Targets

Characteristic	Units	Stack Targets	
		2010	2015
Platinum group metal total content (both electrodes)	g/kW (rated)	0.3	0.2
Platinum group metal (PGM) total loading ^a	mg PGM/cm ² electrode area	0.3	0.2
Cost	\$/kW	5 ^b	3 ^b
Durability with cycling ^c			
Operating temp ≤80°C	h	5,000	5,000
Operating temp >80°C	h	2,000	5,000
Electrochemical area loss ^d	%	<40	<40
Electrocatalyst support loss ^d	mV after 100 hours @ 1.2 V	<30	<30
Mass activity ^e	A/mg Pt @ 900 mV _{IR-free}	0.44	0.44
Specific activity ^e	μA/cm ² @ 900 mV _{IR-free}	720	720
Non-Pt catalyst activity per volume of supported catalyst	A/cm ³ @ 800 mV _{IR-free}	>130	300

^aDerived from performance data at rated power targets specified in Table 3.4.14 of Ref. 2.

^bBased on 2002 dollars, platinum cost of \$450 / troy ounce = \$15/g, loading <0.2 g/kW_e and costs projected to high volume production (500,000 stacks per year).

^cIncludes typical driving cycles.

^dTested per GM protocol (Mathias, M.F., et al., Interface (Electrochemical Society), Fall 2005, p. 24).

^eTest at 80°C/120°C H₂/O₂ in MEA; fully humidified with total outlet pressure of 150 kPa; anode stoichiometry 2; cathode stoichiometry 9.5.

Table 2 describes targets for the membrane. The focus of the targets is to provide guidance for development of membranes that will operate and survive over the entire range of automotive operating conditions. These conditions range from sub-freezing to boiling temperatures and relative humidities of 0 to 100%. For membranes that depend on water for conductivity, freezing or boiling water conditions present obvious problems.

Table 2. Membrane Targets

Characteristic ^a	Units	2010	2015
Oxygen crossover ^b	mA/cm ²	2	2
Hydrogen crossover ^b	mA/cm ²	2	2
<i>Area-specific resistance at:</i>			
Maximum operating temperature and water partial pressures from 40 to 80 kPa	ohm cm ²	0.02	0.02
80 °C water and water vapor partial pressure from 25 to 45 kPa	ohm cm ²	0.02	0.02
30 °C water and water vapor partial pressure up to 4 kPa	ohm cm ²	0.03	0.03
-20°C	ohm cm ²	0.2	0.2
Maximum operating temperature	°C	120	120
Cost ^c	\$/m ²	20	20
Durability with cycling ^d			
Mechanical	Cycles w/<10 sccm crossover	20,000	20,000
Chemical	H ₂ crossover mA/cm ₂	200	20

^aAlternative membranes might need additional tests.

^bTested in MEA at 1 atm O₂ or H₂ at nominal stack operating temperature.

^cBased on 2002 dollars and projected to high-volume production (500,000 stacks per year).

^dIncludes typical driving cycles.

Table 3 contains the targets for the membrane electrode assembly. In addition to the durability and cost targets associated with the electrocatalyst and the membrane, additional performance-related targets pertain to the MEA. Performance is measured in power (watts) per area of cell that can be translated to mass of Pt per watt produced. Pt mass and cost are the primary drivers.

Table 3. Membrane Electrode Assembly Targets

Characteristic	Units	2010	2015
Operating temperature	°C	<120	<120
Inlet water vapor partial pressure	kPa	<1.5	<1.5
Cost ^a	\$/kW	10	5
Durability with cycling ^b			
At operating temp of ≤80 °C	hours	5,000	5,000
At operating temp of >80 °C	hours	2,000	5,000
Unassisted start from low temperature	°C	-40	-40
Performance @ ¼ power (0.8V)	mA/cm ²	300	300
	mW/cm ²	250	250
Performance @ rated power	mW/cm ²	1,000	1,000
Extent of performance (power density) degradation over lifetime ^c	%	10	5
Thermal cyclability in presence of condensed water		Yes	Yes

^aBased on 2002 dollars and costs projected to high volume production (500,000 stacks per year).

^bBased on appropriate test protocol.

^cDegradation target includes factor for tolerance of the MEA to impurities in the fuel and air supply. To be evaluated as a percent decrease in cell voltage at all current densities (i.e., no more than 5%).

Technology Development Approach and Status

Electrocatalyst and Support Research (Figure 2)

Research efforts here are centered on increasing cathode activity and durability. Four strategies are being employed⁶: lower platinum group metal (PGM) content by catalyst particle morphology and crystal structure; Pt alloys with less expensive base metals such as Co, Mn, Ni, and others; novel supports such as non-carbon supports and alternative carbon structures; and non-PGM catalysts.

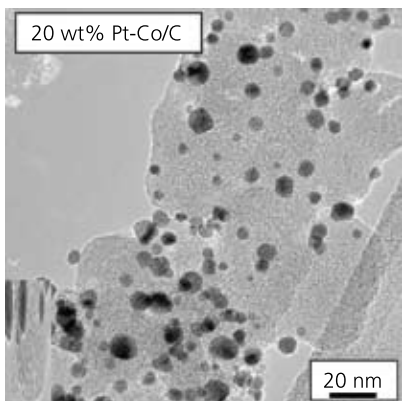


Figure 2. TEM image of a Pt/C electrode. The smaller, darker particles are the Pt catalysts and the larger spherical particles are the carbon supports. Ionomer surrounding the catalyst and support provides a pathway for proton transfer.

An example of a non-carbon catalyst support is 3M's nanostructured thin film polymer whisker concept⁷ as well as titanium oxide (**Aldrich Prod. No. 14021**) and tungsten carbide (**Aldrich Prod. No. 241881**).^{8,9}

Non-PGM catalysts are based on metal porphyrins and other metal-C-N heterocyclic ligand complexes, metal free C-N heterocyclic systems, nitrogen-doped carbon nanostructures and their composites, and metal chalcogenides.¹⁰⁻¹²

Major progress in the electrocatalyst and support area has been made. Several researchers have demonstrated Pt alloy compositions with significantly higher performance and durability than Pt alone.^{10,13,14} A total Pt loading of 0.4 mg Pt/cm² has been demonstrated in a single cell for more than 7,300 hours with voltage cycling, surpassing the 2015 durability targets.¹⁴ Catalysts with the required activity and durability still need to be developed.

Membrane Research

There are two major areas of focus: durability and performance over the entire range of automotive operating conditions. In traditional PFSA membranes, conductivity increases with increasing sulfonic acid group concentration, however this leads to increased swelling and decreases membrane stability. Significant advances in membrane stability have been made in the recent past. Chemical stability has been increased by decreasing the number of carboxylic end groups in the polymer, while mechanical stability has been increased through use of inert support materials, such as PTFE (**Aldrich Prod. Nos. 430935, 430943, 468096, 468118, 182478**), polysulfone (**Aldrich Prod. Nos. 428302, 182443**) or polyimide (**Aldrich Prod. No. 23817**).¹⁵⁻¹⁷ Reinforced membranes have

demonstrated a Young's modulus exceeding 500 MPa at 25°C and 30%RH, compared to ~200 MPa for an unreinforced membrane. Similarly, higher proportional limit stress and higher break stress at all temperature and humidity levels, as well as lower dimensional changes due to swelling were observed for the reinforced membrane.¹⁶ Single cells containing a stabilized MEA have operated for nearly 5,000 hours (the 2015 target) under voltage and humidity cycling.¹⁸ Another single cell with a mechanically stabilized membrane and a Pt-alloy cathode catalyst has recently achieved over 7,300 hours of stable operation with voltage and passive humidity cycling.¹⁴

Projects to address membrane performance under high temperature and low relative humidity operating conditions employ one or more of the following strategies. Phase segregation can be introduced by incorporating separate blocks of hydrophobic and hydrophilic functionality within the same polymer molecule or by producing two-polymer composites in which one polymer provides mechanical strength while the other polymer conducts protons. Non-aqueous proton conductors such as inorganic oxides, heteropolyacids, or ionic liquids enable fuel cell operation at temperatures greater than 100°C. Hydrophilic additives that maintain water content and conductivity at higher temperature are also under consideration.¹⁹ Several researchers have achieved DOE's interim conductivity goal of 70 mS/cm at 30°C and 80% relative humidity.²⁰

Summary

Fuel cell systems are already being demonstrated in prototype vehicles, consumer electronics devices, materials handling equipment, and backup power and other stationary applications. Finally, the performance of the fuel cell system must be comparable in all respects to incumbent technologies, whether it is an internal combustion engine powering an automobile, a diesel generator set providing distributed generation, or a lithium-ion battery powering a consumer electronics device. While many promising new approaches have been developed in the last two years, technical challenges remain to achieve the upcoming 2010 and the ultimate 2015 system targets.

References:

- (1) More, K. 2008 DOE Hydrogen Program Review, Washington, D.C., June 9-13, 2008.
- (2) More, K. 2007 DOE Hydrogen Program Review, Washington, D.C., May 14-19, 2007.
- (3) Yu, P.T., Kocha, S., Paine, L., Gu, W., Wagner, F. AIChE Spring National Meeting: Conference Proceedings, April 25-29, 2004. Publication: New York, NY: American Institute of Chemical Engineers, - Standard No: ISBN: 0816909423 (CD-ROM).
- (4) US Department of Energy. Information Resources. <http://www.eere.energy.gov/hydrogenandfuelcells/mypp> (accessed Oct 24, 2008).
- (5) Motupally, S., International Workshop on Degradation Issues of Fuel Cells, September 2007, Crete, Greece.
- (6) Payne, T.L., Benjamin, T.G., Garland, N.L., Kopasz, J.P. *ECS Trans.*, 2008, 16, in press.
- (7) Debe, M. 2007 DOE Hydrogen Program Review, Washington, D.C., May 14-18, 2007.
- (8) Viswanathan, V. 2008 DOE Hydrogen Program Review, Washington, D.C., June 9-13, 2008.
- (9) Merzougui, B., Carpenter, M.K., Swathirajan, S., U.S. Patent 20060257719, 2006.
- (10) Protsailo, L. in DOE Hydrogen Program 2005 Annual Progress Report, p. 739, U.S. Department of Energy, Washington D.C., 2005.
- (11) Shao, Y., Sui, J., Yin, G., and Gao, Y., *Appl. Catal. B-Environ.*, 2008, 79, 89.
- (12) Zhang, L., Zhang, J., Wilkinson, D.P., Wang, H., *J. Power Sources*, 2006, 156, 171.
- (13) Zelenay, P. 2008 DOE Hydrogen Program Review, Washington, D.C., June 9-13, 2008.
- (14) Debe, M. 2008 DOE Hydrogen Program Review, Washington, D.C., June 9-13, 2008.
- (15) Schwiebert, K.E., Raiford, K.G., Escobedo, G., Nagarajan, G., *ECS Trans.*, 2006, 1, 303.
- (16) Tang, Y., Kusoglu, A., Karlsson, A.M., Santare, M.H., Cleghorn, S., Johnson, W. B., *J. Power Sources*, 2008, 175, 817.
- (17) Mittelsteadt, C. 2008 DOE Hydrogen Program Review, Washington, D.C., June 9-13, 2008.
- (18) Escobedo, G., Barton, K., Choudhury, B., Curtin, D., Perry, R. 2007 Fuel Cell Seminar & Exposition, San Antonio, TX, p. 20, 2007.
- (19) Martin, K.E., Garland, N.L., Kopasz, J.P., McMurphy, K.W. 236th ACS National Meeting, Philadelphia, PA, August 17-21, 2008.
- (20) Fenton, J. 2008 DOE Hydrogen Program Review, Washington, D.C., June 9-13, 2008.

Catalyst Materials for PEM Fuel Cells

For a complete list of fuel cell catalysts please visit sigma-aldrich.com/catalyst.

Platinum Group Metals on Carbon Support

Name	Metal Loading	Matrix	Cat. No.
Palladium on carbon	loading 5 wt. %	carbon powder, wet support	520845-10G 520845-50G
	loading 5 wt. % (dry basis)	carbon, wet support	520837-10G
	loading 3 wt. %	activated carbon support	237515-10G 237515-50G
	loading 1 wt. %	activated carbon support	205672-25G 205672-100G
Platinum on activated charcoal	10% Pt basis (based on dry substance)	activated charcoal support, moistened with water (H ₂ O ~50%)	80983-1G 80983-5G
	5% Pt basis	activated charcoal support	80982-5G 80982-25G
	10% Pt basis	activated charcoal support	80980-1G 80980-5G
Platinum on carbon	loading 1 wt. %	activated carbon support	205923-5G 205923-25G
Ruthenium on carbon	loading 5 wt. %	carbon support	206180-25G 206180-100G

Platinum Group Metals on Non-Carbon Support

Name	Metal Loading	Description	Cat. No.
Palladium on alumina	loading 1 wt. %	powder	205702-25G
Palladium on barium carbonate	loading 5 wt. %	reduced	237523-10G
Palladium on calcium carbonate	loading 5 wt. %	unreduced	214353-10G 214353-50G
Platinum on alumina	loading 5 wt. %	powder	205974-10G 205974-50G
	loading 1 wt. %	powder	205966-25G 205966-100G

Unsupported Platinum Group Metals

Name	Purity	Description	Cat. No.
Platinum black	99.9+%	powder, surface area ~25 m ² /g	205915-250MG 205915-1G 205915-5G
	99.9+% trace metals basis, fuel cell grade	powder, surface area 25-34 m ² /g	520780-1G 520780-5G
	99.9+%	powder, surface area 20-25 m ² /g	520802-1G 520802-5G
	99.9+% trace metals basis	powder, surface area 27-36 m ² /g	520799-1G 520799-5G
Ruthenium black	≥98%	powder, surface area 17-26 m ² /g	326712-1G

Membrane Materials for PEM Fuel Cells

For a complete list of membrane materials including silica-composite membranes, please visit sigma-aldrich.com/membranes.

Membranes

Name	Equivalent Weight	Dimensions	Cat. No.
Nafion® 350, perfluorinated membrane, reinforced with PTFE	-	L × W 8 × 10 in. thickness 0.01 in.	454737-1EA
Nafion perfluorinated membrane	eq. wt. 1,100	L × W 12 × 12 in. thickness 0.005 in.	541346-1EA
Nafion perfluorinated membrane	eq. wt. 1,100	L × W 8 × 10 in. thickness 0.007 in.	274674-1EA
Nafion perfluorinated membrane	eq. wt. 1,100	L × W 12 × 12 in. thickness 0.007 in.	292567-1EA
Nafion perfluorinated membrane, reinforced with poly(tetrafluoroethylene) fiber	A 'bimembrane' with one layer having equivalent weight 1,500 and thickness 0.001 in., and the other layer having equivalent weight 1,000 and thickness 0.005 in.	L × W 12 × 12 in. thickness 0.006 in.	565067-1EA
Nafion perfluorinated membrane, reinforced with poly(tetrafluoroethylene) fiber	eq. wt. 1,100	L × W 12 × 12 in. thickness 0.007 in.	563994-1EA
Nafion perfluorinated membrane, reinforced with poly(tetrafluoroethylene) fiber	eq. wt. 1,050	L × W 12 × 12 in. thickness 0.005 in.	564664-1EA
Nafion perfluorinated membrane	eq. wt. 1,100	L × W 12 × 12 in. thickness 0.002 in.	676470-1EA

Solutions & Dispersions

Name	Concentration	Equivalent Weight	Cat. No.
Nafion 117	~ 5% in a mixture of lower aliphatic alcohols and water	-	70160-25ML 70160-100ML
Nafion perfluorinated resin	5 wt. % in mixture of lower aliphatic alcohols and water, water 45%	eq. wt. 1,000	527084-25ML 527084-100ML
Nafion perfluorinated resin	5 wt. % in mixture of lower aliphatic alcohols and water, water 45%	eq. wt. 1,100	510211-25ML 510211-100ML
Nafion perfluorinated resin	20 wt. % in lower aliphatic alcohols and water, water 34%	-	663492-25ML 663492-100ML
Nafion perfluorinated resin	20 wt. % in mixture of lower aliphatic alcohols and water, water 20%	eq. wt. 1,100	527122-25ML 527122-100ML
Nafion perfluorinated resin	5 wt. % in lower aliphatic alcohols and water, water 15-20%	eq. wt. 1,100	274704-25ML 274704-100ML 274704-500ML
Nafion perfluorinated resin, aqueous dispersion	10 wt. % in H ₂ O	eq. wt. 1,000	527114-25ML 527114-100ML
Nafion perfluorinated resin, aqueous dispersion	10 wt. % in H ₂ O	eq. wt. 1,100	527106-25ML 527106-100ML
Poly(styrene- <i>ran</i> -ethylene), sulfonated, cross-linkable	5 wt. % in 1-propanol	-	659401-25ML 659401-100ML
Polystyrene- <i>block</i> -poly(ethylene- <i>ran</i> -butylene)- <i>block</i> -polystyrene, sulfonated	5 wt. % in 1-propanol and dichloroethane	-	448885-25ML 448885-100ML
Polystyrene- <i>block</i> -poly(ethylene- <i>ran</i> -butylene)- <i>block</i> -polystyrene, sulfonated, cross-linkable	5 wt. % in 1-propanol and dichloroethane	-	659444-25ML 659444-100ML

Other Membrane Materials

Name	Form	Mol. Wt./ Eq. Wt	Cat. No.
Nafion NR50	pellets	eq. wt. ≤1250	309389-10G 309389-25G
Nafion perfluorinated resin, powder	powder	eq. wt. 1,100	495786-500MG
Nafion SAC-13	fluorosulfonic acid Nafion® polymer on amorphous silica 10-20% (porous nanocomposite)	-	474541-10G 474541-25G
Poly(vinylphosphonic acid)	powder	-	661740-1G
Poly(2-vinylpyridine-co-styrene)	granular	average M _n ~130,000 average M _w ~220,000 by LS	184608-25G 184608-50G

Electrode Materials for Solid Oxide Fuel Cells (SOFC)

For a complete list of electrode materials please visit sigma-aldrich.com/fuelcell.

Anode Materials

Name	Description	Composition	Cat. No.
Nickel oxide - Cerium samarium oxide	NiO/SDC for coatings	Cerium Samarium Oxide 40 wt. % Nickel Oxide 60 wt. %	704210-10G
Nickel oxide - Yttria-stabilized zirconia	NiO/YSZ for coatings	Nickel Oxide 66 wt. % Yttria-Stabilized Zirconia 34 wt. %	704202-10G
Nickel oxide - Yttria-stabilized zirconia	NiO/YSZ general applications	Nickel Oxide 60 wt. % Yttria-Stabilized Zirconia 40 wt. %	704229-10G

Cathode Materials

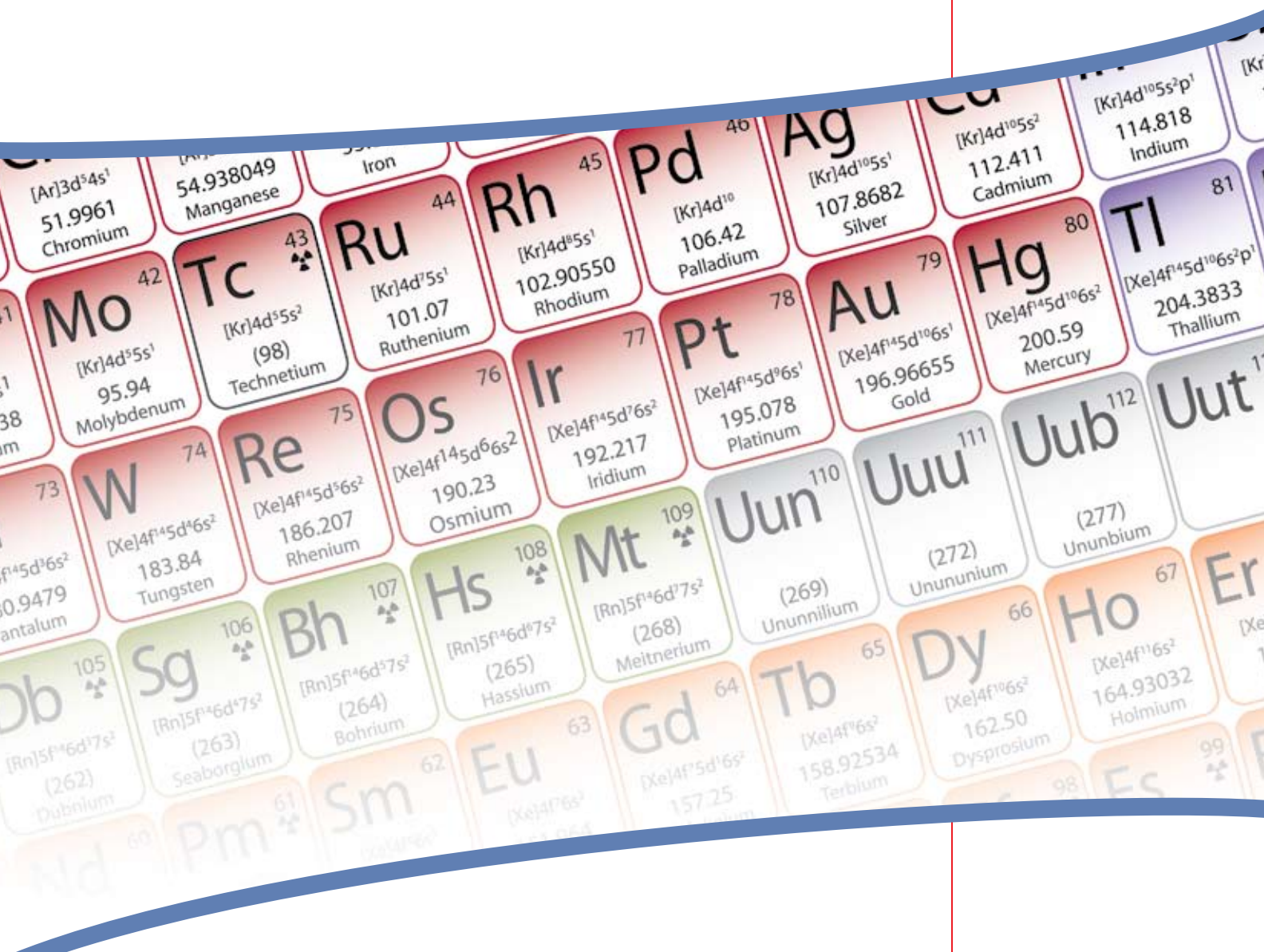
Name	Description	Composition	Cat. No.
Lanthanum strontium cobalt ferrite	LSCF 6428	$\text{La}_{0.6}\text{Sr}_{0.4}\text{Co}_{0.2}\text{Fe}_{0.8}\text{O}_3$	704288-10G
Lanthanum strontium cobalt ferrite	LSCF/GDC composite cathode powder	$(\text{Ce}_{0.5}\text{Gd}_{0.1})\text{O}_{1.95}$ 50% $(\text{La}_{0.6}\text{Sr}_{0.4})\text{Co}_{0.2}\text{Fe}_{0.8}\text{O}_3$ 50%	704253-10G
Lanthanum strontium manganite	LSM-20/YSZ composite cathode powder	$(\text{La}_{0.8}\text{Sr}_{0.2})\text{MnO}_3$ 50% $(\text{Y}_2\text{O}_3)_{0.08}(\text{ZrO}_2)_{0.92}$ 50%	704245-10G
Lanthanum strontium manganite	LSM-35	$\text{La}_{0.6}\text{Sr}_{0.35}\text{MnO}_3$	704261-10G
Lanthanum strontium manganite	LSM-20	$(\text{Ce}_{0.5}\text{Gd}_{0.1})\text{O}_{1.95}$ 50% $(\text{La}_{0.8}\text{Sr}_{0.2})\text{MnO}_3$ 50%	704296-10G
Lanthanum strontium manganite	LSM20-GDC10	$\text{La}_{0.8}\text{Sr}_{0.2}\text{MnO}_3$	704237-10G

Electrolyte Materials for Solid Oxide Fuel Cells (SOFC)

For a complete list of electrolyte materials please visit sigma-aldrich.com/fuelcell.

Name	Additives	Particle Size	Surface Area	Cat. No.
Cerium(IV) oxide-calcium doped	calcium 10 mol % as dopant	<100 nm	surface area 100-120 m ² /g	572403-25G
Cerium(IV) oxide-gadolinium doped	gadolinium 20 mol % as dopant	<100 nm	surface area >100 m ² /g	572357-25G
	gadolinium 10 mol % as dopant	<100 nm	surface area >100 m ² /g	572330-25G
Cerium(IV) oxide-samarium doped	samarium 15 mol % as dopant	<100 nm	surface area 100-120 m ² /g	572365-25G
Cerium(IV) oxide-yttria doped	yttria 15 mol % as dopant	<100 nm	surface area 100-120 m ² /g	572381-25G
Cerium(IV)-zirconium(IV) oxide	-	<50 nm (BET)	-	634174-25G 634174-100G
Zirconium(IV) oxide-yttria stabilized	Y ₂ O ₃ 0-10% as stabilizer	<100 nm (BET)	BET surf. area 40-60 m ² /g	544779-5G 544779-25G
	yttria 3% as stabilizer	≤100 nm	surface area 100-120 m ² /g	572322-25G
	yttria 8% as stabilizer	≤100 nm	surface area >100 m ² /g	572349-25G
	yttria ~8% as stabilizer	~700 nm	surface area 5.5 m ² /g	464228-100G 464228-500G
	yttria ~5.3% as stabilizer	~500 nm	surface area 6.9 m ² /g	464201-100G 464201-500G

Interactive Periodic Table



A roadmap to Aldrich Materials Science Products on the Web.

Click on your metal of interest to see major product groups.

- Metals
- Metal Oxides
- Salts
- Nanomaterials
- Organometallic Precursors

Visit the Interactive Periodic Table at sigma-aldrich.com/periodic

All 61 non-radioactive metals in the periodic table are available from Sigma-Aldrich.

Polymer-based Materials for Printed Electronics: Enabling High Efficiency Solar Power and Lighting



Ritesh Tipnis*, Darin Laird and Mathew Mathai
Plextronics, Inc.
2180 William Pitt Way
Pittsburgh, PA 15238
*Email: rtipnis@plextronics.com

Introduction

The soaring global demand for energy has created an urgent need for new energy sources that are both cost-competitive and eco-friendly. Renewable energy technology, such as solar power and energy efficient solid-state lighting (SSL), could help satisfy these pressing needs. Solar power, however, is not widely commercialized because the cost of today's silicon-based technology often limits its use mainly to large, on-grid applications. Similarly, the complex and expensive processes required for current SSL technologies have inhibited wide-scale deployment.

Printed electronics (PE) holds the promise of enabling low-cost, scalable solutions to address the issues faced by today's solar and SSL technologies. PE exploits the ability of organic materials to be solution processed onto large area substrates at a fraction of the manufacturing cost associated with conventional vapor deposition techniques. As such, low-cost applications in lighting, power and circuitry are expected to fuel the growth of the PE industry from the current \$1 billion to a \$300 billion market in the next 20 years.¹ Plextronics, Inc. is helping seed this market by developing materials for applications in organic photovoltaic (OPV) devices and organic light emitting diodes (OLED), with eventual applications in solar power and SSL.

Organic Light Emitting Diodes

In 2001, the energy consumption for lighting in buildings within the US was 8.2 quads (1 quad = 1.055×10^{18} joules), representing 22% of the total energy consumed.² It is forecasted that efficient lighting can reduce 3.5 quads of electricity consumption by 2025. This translates to 41 less 1000 MW power plants, resulting in tremendous economic and environmental benefits. Solid-state white lighting, driven by OLED technology, can help realize this vision with energy efficient products to replace fluorescent lighting sources for general illumination beginning in 2010. There also exists significant opportunity for implementation in diffuse lighting applications that require flexibility, color tunability and low energy consumption.

The display industry has already begun to employ OLED materials in applications such as cell phones, mp3 players, and, most recently, televisions.³ However, significant market penetration remains elusive because performance parameters, such as device efficiency, lifetime, and operating voltage, require further optimization. In addition, considerable capital investment is required to retrofit manufacturing lines, which today use a series of vacuum-deposition processes for each color. Utilizing a manufacturing process based on solution processing will enable significantly higher materials' utilization and lower energy consumption, whilst being cost-effective. Also, the use of an effective, solution-processable Hole Injection Layer (HIL) in the device stack directly impacts the performance of the device. An HIL enables efficient hole injection between the electrode and the neighboring light emitting/transport layers by reducing the energy barriers between the electrode and the semiconducting layer.⁴ Improved hole injection implies the capability to modulate the charge balance within the device, which in turn improves device lifetime. In addition, the effective reduction of energy barriers at interfaces lowers the operating voltage for OLEDs and also results in superior luminescent performance.⁵ Besides these functions, the HIL also planarizes the anode surface to prevent shorts, and blocks electrons from flowing out of the emitting layer and into the anode without recombination.⁶ All of these factors contribute to improvements in OLED performance, leading up to a commercially viable technology.

Organic Photovoltaics

A typical US coal-power plant emits, per GWh, about 1000 tons of CO₂, 8 tons of SO₂, 3 tons of NO_x, and 0.4 tons of particulates.⁷ This has led to legitimate environmental concerns, which renewable energy sources like solar power can mitigate. However, today's solar technology does not provide a clear path to meet the soaring demand. At the same time, the current primary source of solar technology, silicon-based solar energy, has not proven to be cost-effective due to significant raw material costs as well as the high infrastructure cost. The leveled cost of power from today's solar installations is as much as ten times that of grid-supplied power depending on size of installation and geographical location. Second generation PV devices based on thin films of amorphous silicon, cadmium telluride (CdTe) or copper indium gallium diselenide (CIGS) are relatively inexpensive compared to silicon, but have not yet achieved wide scale adoption because they are still not cost competitive with grid pricing.

Polymer based OPV cells offer the potential to play a significant role as a zero-emission source of energy during the actual power generation process. However wide-scale commercialization requires a pathway towards large-scale, economical manufacturing. While low costs of raw materials and less complex manufacturing represent a major advantage in comparison to the currently dominant silicon-based solar cells, gains in efficiency are necessary to enable commercialization of OPV. Polymer-fullerene p-n junction (PNJ) solar cells are a promising approach to achieve such performance gains.

Materials for Printed Electronics

Polymer Semiconductors

Plextronics' Plexcore® technology platform is comprised of semiconducting polymers and solution-processable inks that are designed to maximize the efficiency, lifetime and stability of PE devices. Plexcore OS, in particular, is a p-type organic semiconductor based on regioregular poly 3-hexylthiophene, RR-P3HT (**Figure 1**), a semi-crystalline, semiconducting polymer with exceptional spectroscopic and electronic properties. The material is easily synthesized via a method developed by Plextronics' co-founder, Dr. Richard D. McCullough.⁸⁻¹¹ Plexcore OS 2100 (**Aldrich Prod. No. 698997**) is a grade of P3HT specifically designed for OPV and demonstrates the following properties:

- Electronics grade purity (<15 ppm metals) and high regioregularity enables high OPV performance through efficient light harvesting and hole transport.
- Readily formulated into printable inks with tailored material properties for a wide range of electronic applications.
- Consistent material supply via large-scale production provides minimized device and processing variability.

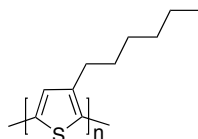


Figure 1. Poly 3-hexylthiophene (**Aldrich Prod. Nos. 698997, 698989**)

Data from recent batches of Plexcore OS 2100 demonstrate a production process that delivers consistent material properties batch-to-batch. **Figures 2 and 3** provide batch-to-batch data for molecular weight (MW)/polydispersity index (PDI) and the metals content, respectively. Appropriate nanoscale morphology of thin films of RR-P3HT is required to achieve high charge carrier mobilities, a key factor in enabling efficient OPV device performance. Regioregularity, MW, and PDI are all known to influence this morphology, where, in general, high MW and low PDI deliver world-class performance. Maintaining these material properties in a controlled production process enables the end user to develop reproducible material processing and device fabrication. As such, variability is minimized to enable development focus in other areas such as device architecture.

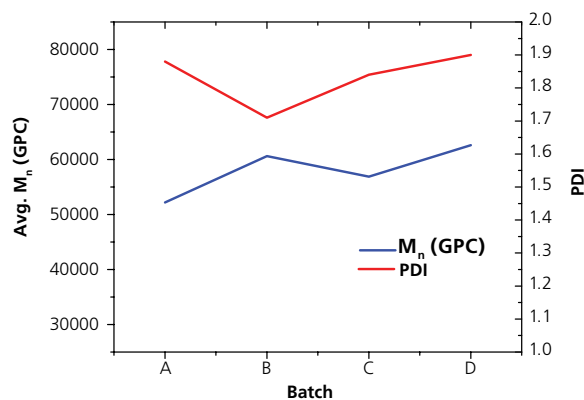


Figure 2. Plexcore OS 2100 example batch data—molecular weight (left) and PDI (right).

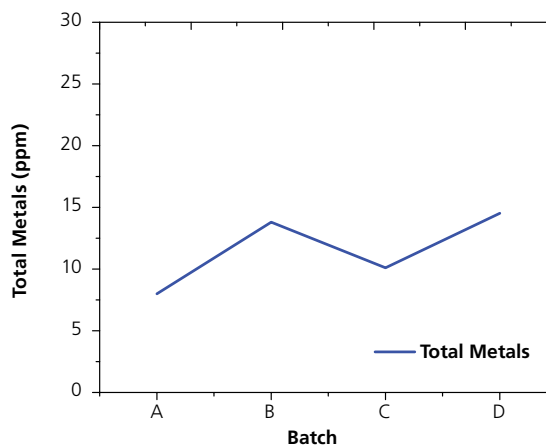


Figure 3. Plexcore OS 2100 example batch data—total metals

The metals content of organic materials has not been comprehensively studied to determine the impact on OPV performance. It is believed, however, that higher metals content may result in increased charge trapping within the thin film, which may lower charge carrier mobility, resulting in poor device performance. Within the OLED industry, metals content has been known to cause degradation and reduced device efficiency and lifetime. As such, Plextronics focuses on delivering materials with electronics-grade purity to minimize and eliminate potentially detrimental degradation mechanisms due to material purity. The combination of these properties leads to consistency in the performance of OPV devices fabricated with different batches of Plexcore OS 2100, as seen in **Figure 4**.

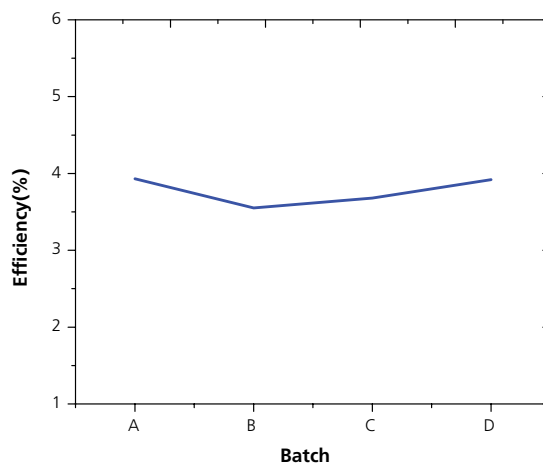


Figure 4. OPV efficiency for P3HT:PCBM. Plexcore OS 2100 example batch data demonstrating OPV performance

The PNJ solar cell consists of an active layer that is a composite of a p-type (electron donating) light harvesting polymer and an n-type (electron accepting) semiconductor. **Figure 5** shows the basic device architecture for an OPV cell comprising a photoactive layer. For the purposes of this discussion, the photoactive layer is based on a blend of Plexcore® OS 2100 (P3HT) and [6,6] phenyl C₆₁ butyric acid methyl ester (PCBM), deposited on top of an organic hole transport layer (HTL), that planarizes the transparent anode, and also facilitates the collection of positive charge carriers (holes) from the light-harvesting layer. These photo-generated charges migrate to the collecting electrodes through this intimately mixed interpenetrating network. Examples of the best performing polymer organic cells have been based on the P3HT:PCBM junction.¹²⁻¹⁵ The system is characterized by phase-separation of the p- and n-components of the composite into discrete manifolds beneficial for charge transport and exciton dissociation. The I-V data in **Figure 6** represents a single-junction OPV cell that was certified by the National Renewable Energy Laboratory (NREL) at 3.39% efficiency; a typical performance in a P3HT:PCBM system.

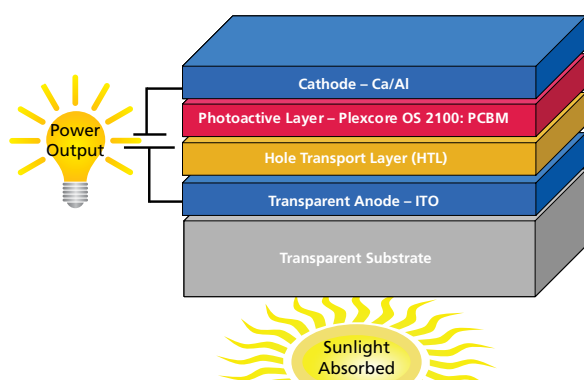


Figure 5. OPV device stack.
ITO: Indium Tin Oxide
PCBM: [6,6] phenyl C₆₁ butyric acid methyl ester
Ca/Al: Calcium/Aluminium

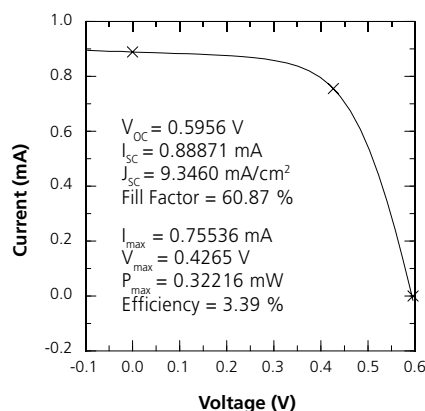


Figure 6. NREL certified I-V curve for Plexcore OS 2100:PCBM OPV cell. The device temperature is $27.0 \pm 3.0 \text{ }^\circ\text{C}$, the device area is 0.095 cm^2 and the irradiance is 1000.0 W/m^2 .

Several material parameters directly impact short circuit current density (J_{sc}), open circuit voltage (V_{oc}), fill factor (FF), and ultimately the efficiency (η) of an OPV device, as depicted in **Table 1**. V_{oc} is a measure of cell potential and typically scales with the difference between lowest unoccupied molecular orbital (LUMO) level of the n-type semiconductor and the

highest occupied molecular orbital (HOMO) level of the p-type semiconductor. J_{sc} is a measure of the maximum current density that could, in practice, be produced by a cell. It is principally influenced by the band-gap of the light-harvesting organic materials in an OPV device. Power In is typically defined as 1000 W/m^2 , which is equivalent to 1 sun (AM 1.5G). Conjugated polymers have strong, broad light absorption and most are semiconducting materials that exhibit a range of band gaps. FF is a figure of merit for how much power the cell can output versus the ideal power defined by the J_{sc} and V_{oc} product. Many material properties, such as nanoscale morphology and charge carrier mobilities of the electrons and holes, affect the photophysical processes in an OPV cell. When optimized, this process leads to efficient charge separation and extraction; and FF is a composite parameter that includes contributions from all of these processes. Achieving > 7% cell efficiencies will require tailoring of all of these properties in combination. In addition, advancements in packaging, device architecture, and electrode engineering will contribute to the best performance of organic solar cells for commercial applications. Plextronics is actively pursuing development of higher efficiencies with the Plexcore PV platform. NREL-certified efficiencies in excess of 5% have already been achieved with improvements in materials and morphology.¹⁶

$$\eta = V_{oc} * J_{sc} * FF / \text{Power In}$$

Table 1. Factors Influencing OPV Efficiency

Drivers of Efficiency	Material and Ink Properties
V_{oc} (V) Open Circuit Voltage	<ul style="list-style-type: none"> Molecular Energies LUMO_{n-type}-HOMO_{p-type}
J_{sc} (mA/cm ²) Short Circuit Current Density	<ul style="list-style-type: none"> E_g (Band gap) α (Absorption coefficient) Charge Extraction
FF Fill Factor	<ul style="list-style-type: none"> p/n charge carrier mobility balance Bulk Heterojunction Morphology

Polymer Conductors

Regioselective polymerization techniques used for synthesizing P3HT allow fine control of the absolute structure of the polymeric materials which support a variety of functionalities, thus enabling a greatly expanded platform for polymer design.¹⁷ For example, Plextronics has developed an inherently doped sulfonated solution of Poly(thiophene-3-[2-(2-methoxyethoxy)ethoxy]-2,5-diyl) (see **Figure 7**). When combined with a matrix polymer and other additives in a solvent system, this ink formulation functions as an effective hole injection layer (HIL) for OLED devices¹⁸ and as a hole transport layer (HTL) for OPV devices. Plextronics provides 2% concentration solutions for application as an HIL - Plexcore OC 1100 (**Aldrich Prod. No. 699799**) and Plexcore® OC 1200 (**Aldrich Prod. No. 699780**).

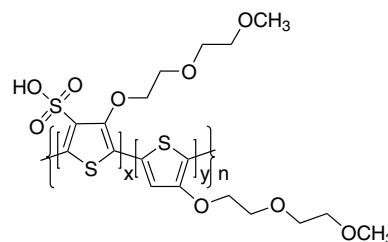


Figure 7. Poly(thiophene-3-[2-(2-methoxyethoxy)ethoxy]-2,5-diyl), sulfonated (**Aldrich Prod. Nos. 699799, 699780**)

Some of the performance benefits that Plexcore® OC offers as an HIL include:

- Reduced acidity, preventing anode degradation and ensuring improved device lifetime.
- Tunable properties such as work function, resistivity, surface energy, and viscosity, enabling researchers to optimize device performance.
- Compatible with multiple solvent systems and aqueous-based solutions, facilitating a variety of processing techniques.

The ability to solution process the HIL presents several advantages, including broad materials selection, flexibility in molecular design, lower materials consumption and processability at ambient temperature and atmospheric pressure. One of the unique features of Plexcore OC inks is the ability to be tuned to match the work function, resistivity, and viscosity, for example, required for specific device architectures and application techniques. This tunability provides the versatility needed to develop new solid state lighting (SSL) device stacks.

Figure 8 shows a typical Phosphorescent LED (PHOLED) device architecture where the HIL layer, such as Plexcore OC 1100 or 1200, is deposited onto the anode via spin coating. **Figure 9** shows representative performance data for a green PHOLED made using Plexcore OC. The turn-on voltage of the device is at the band gap of the emitter, indicating low interfacial energy barriers, which could be attributed to efficient hole injection. This leads to efficiencies as high as 14-15 cd/A being obtained in a PHOLED device architecture, with modest efficiency loss as the current density is increased.

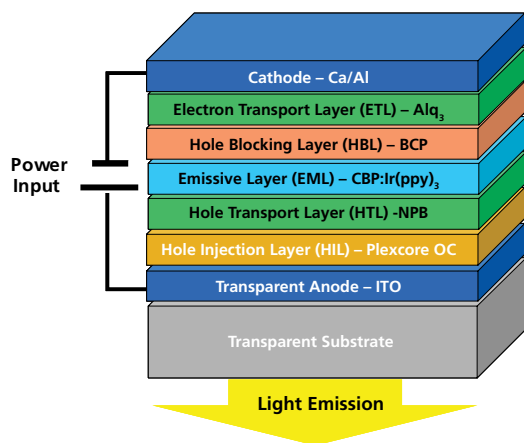


Figure 8. OLED device stack

ITO: Indium Tin Oxide (see table on page 98)

NPB: *N,N'*-Bis(naphthalen-1-yl)-*N,N'*-bis(phenyl)benzidine

(Aldrich Prod. No. 556696)

CBP: 4,4'-*N,N'*-dicarbazole-biphenyl (Aldrich Prod. No. 699195)

Ir(ppy)₃: *tris*-[2-phenylpyridinato-C₂,N]iridium(III) (Aldrich Prod. No. 694924)

BCP: 2,9-dimethyl-4,7-diphenyl-1,10-phenanthroline (bathocuproine)

(Aldrich Prod. No. 699152)

Alq₃: *tris*-8-hydroxyquinoline aluminium (Aldrich Prod. No. 697737)

Ca/Al: Calcium/Aluminium

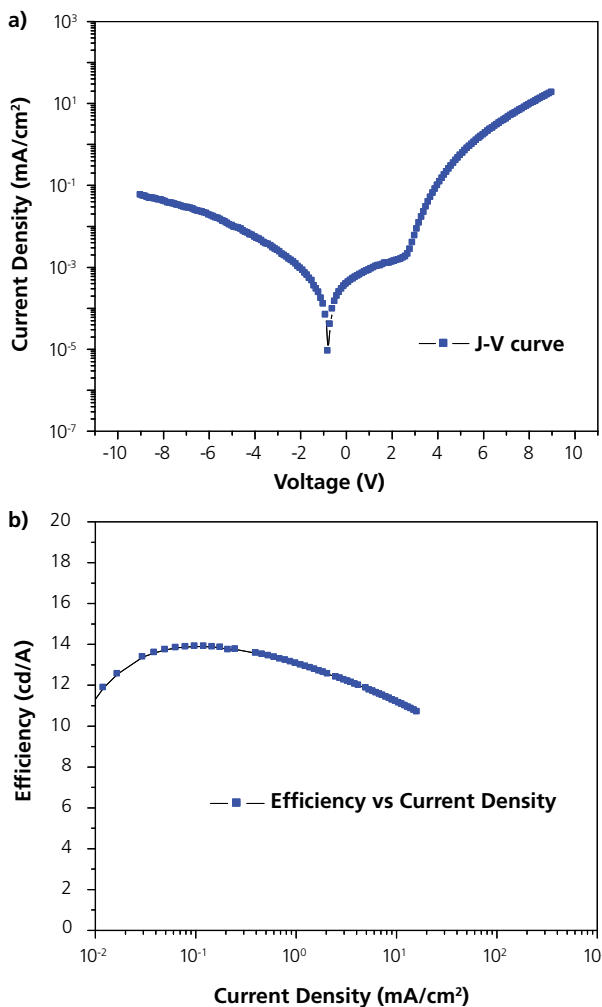


Figure 9. (a) J-V curve; (b) efficiency vs. current density for a green PHOLED with device architecture shown in Figure 8.

One of the critical aspects for a SSL luminaire is the ability to achieve high brightness at low operating voltage. **Figure 10** shows the power efficiency of the device shown on the previous page as a function of operating brightness. The presence of the HIL reduces injection barriers leading to lower operating voltage and improved efficacy (Lumen/Watt) at higher brightness. Maintaining higher efficacy at higher brightness ensures more light output for lower cost. It is expected that SSL products enabled by Plexcore® OC will help realize the energy efficient lighting of the future.

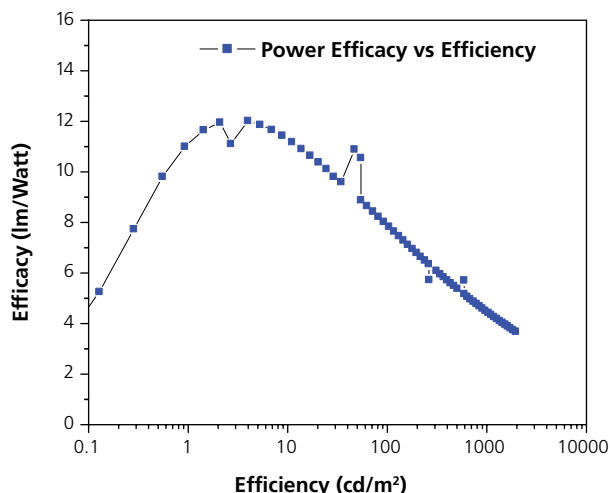


Figure 10. Power efficiency of a PHOLED utilizing Plexcore OC as the hole injection layer (HIL). As observed, the loss in power efficacy is minimized up to 1,000 units of brightness.

Conclusion

Printed Electronics could dictate the future of electronics and the energy industry by employing OPV and OLED devices in various applications, such as solar modules and luminaires based on solid state lighting. In addition, applications that integrate light and power may enable a new market segment for economical and environmentally friendly products. Plextronics' polymer products such as Plexcore OS have the potential to yield high-efficiency OPV devices to serve the renewable energy market. Also, Plexcore OC ink systems that have already demonstrated exceptional performance in OLED devices, can enable SSL products and help meet the low energy consumption demands of the lighting market.

References:

- (1) Nanomarkets, *Organic Electronics: A Market & Technology Assessment*. **2007**
- (2) Navigant, *DOE, Lighting Research & Development Report 2006*. (3) Sony Corporation. www.sonystyle.com (accessed Oct 24, 2008).
- (4) Gong, X. M. D., Moses, D., Heeger, A. J., Liu, S., Jen, K. *Appl. Phys. Lett.* **2003**, *83*, 183.
- (5) Chen, S., Wang, C. *Appl. Phys. Lett.* **2005**, *85*, 765.
- (6) Kraft, A., Grimsdale, A. C., Holmes, A. B. *Angew. Chem. Int. Ed.* **1998**, *37*, 402.
- (7) Fthenakis, V. M. In *European Materials Research Society Spring Meeting*, Nice, France, May 29-June 2. **2006**.
- (8) McCullough, R. D., Lowe, R. S. *J. Chem. Soc., Chem. Commun.* **1992**, 70.
- (9) McCullough, R. D., Lowe, R. S., Jayaraman, M., Anderson, D. L. *J. Org. Chem.* **1993**, *58*, 904.
- (10) McCullough, R. D., Lowe, R. S., Jayaraman, M., Ewbank, P. C., Anderson, D. L., Tristram-Nagle, S. *Synth. Met.* **1993**, *55*, 1198.
- (11) McCullough, R. D., Williams, S. P., Tristram-Nagle, S., Jayaraman, M., Ewbank, P. C., Miller, L. *Synth. Met.* **1995**, *67*, 279.
- (12) Kazmerski, L. L. *J. Electron Spectrosc. Relat. Phenom.* **2006**, *150*, 105.
- (13) Li, G., Shrotriya, V., Huang, J., Yao, Y.; Moriarty, T., Emery, K., Yang, Y. *Nature Materials* **2005**, *4*, 864.
- (14) Ma, W., Yang, C., Gong, X., Lee, K.; Heeger, A. J. *Adv. Funct. Mater.* **2005**, *15*, 1617.
- (15) Reyes-Reyes, M., Kim, K., Carroll, D. L. *Appl. Phys. Lett.* **2005**, *87*, 083506.
- (16) Green, M. A., Emery, K., Hishikawa, Y., Warta, W. *Prog. Photovolt: Res. Appl.* **2008**, *16*, 435.
- (17) Lowe, R. S., Khersonsky, S. M., McCullough, R. D. *Adv. Mater.* **1999**, *11*, 250.
- (18) Shao, Y., Sui, J., Yin, G., and Gao, Y., *Appl. Catal. B-Environ.*, **2008**, *79*, 89.

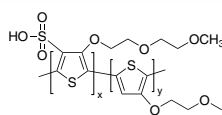
Organic Electronic Materials: Plexcore Products

Poly(3-hexylthiophene-2,5-diyl)-Electronic Grade

Application	Structure	Purity	Description	Cat. No.
High molecular weight; ultra-high purity P3HT optimized for use in organic photovoltaics (OPV) research and devices.		99.995% trace metals basis, >98% head-to-tail regioregular (HNMR)	average M _n , 45,000-65,000	698997-250MG 698997-1G
High purity P3HT for organic electronics research. Material optimized for use in active layers of OFETs and other devices.		99.995% trace metals basis, >95% head-to-tail regioregular (HNMR)	average M _n , 25,000-35,000	698989-250MG 698989-1G

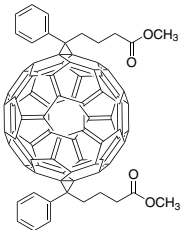
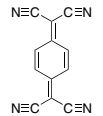
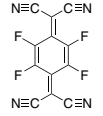
Poly(thiophene-3-[2-(2-methoxyethoxy)ethoxy]-2,5-diyl), sulfonated solution-Electronic Grade

Plexcore OC 1100 (**699799**) and 1200 (**699780**) are organic conductive inks suitable for spin coating applications and as hole injection layers in organic electronic devices.

Structure	Purity	Description	Cat. No.
	≥99.99% trace metals basis	2% in ethylene glycol monobutyl ether/water, 3:2	699780-25ML
	≥99.99% trace metals basis	2% in 1,2-propanediol/isopropanol	699799-25ML

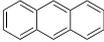
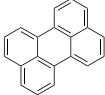
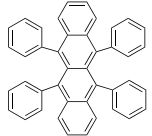
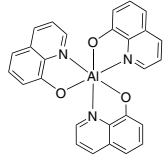
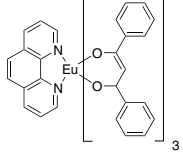
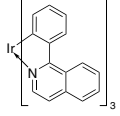
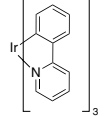
Electron Acceptors

For a complete list of electron acceptors and to view the PCBM library, please visit sigma-aldrich.com/oel.

Name	Structure	Purity	Cat. No.
[6.6] Diphenyl C ₆₂ bis(butyric acid methyl ester)(mixture of isomers)		99.5%	704326-100MG
7,7,8,8-Tetracyanoquinodimethane		98%	157635-1G 157635-5G 157635-10G
2,3,5,6-Tetrafluoro-7,7,8,8-tetracyanoquinodimethane		97%	376779-5MG 376779-25MG

Organic Photovoltaics Materials: Light-Emitters and Dopants-Sublimed Grade*

For a complete list of light-emitters and dopants please visit sigma-aldrich.com/oel.

Name	Structure	Purity	Absorption/ Fluorescence ($\lambda_{ex}/\lambda_{em}$)	Cat. No.
Anthracene, sublimed grade		≥99%	-	694959-5G 694959-25G
Perylene, sublimed grade		≥99.5%	-	394475-1G 394475-5G
Rubrene, sublimed grade		-	λ_{max} 299 nm	551112-100MG 551112-500MG
Tris(8-hydroxyquinoline)aluminum, sublimed grade		99.995% trace metals basis	390 / 519 nm	697737-1G
Tris(dibenzoylmethane) mono(1,10-phenanthroline)europium(III), sublimed grade		-	λ_{max} 228 nm, 355 / 615 nm in tetrahydrofuran	538965-250MG
Tris[1-phenylisoquinoline-C ² ,N]iridium(III), sublimed grade		99%	324 / 615 nm in tetrahydrofuran	688118-250MG
Tris[2-phenylpyridinato-C ² ,N]iridium(III), sublimed grade		-	305 / 507 nm in chloroform	694924-250MG

*TGA/DSC Lot specific traces available upon request

Organic Photovoltaic Materials: Indium Tin Oxide/Indium Oxide

For a complete list of ITOs please visit sigma-aldrich.com/oel.

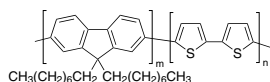
Indium Tin Oxide/Indium Oxide Coated Slides & PET Sheets

Product Description	Surface Resistivity	Cat. No.
Indium tin oxide coated glass slide	8-12 Ω/sq	703192-10PAK
Indium tin oxide coated glass slide	30-60 Ω/sq	703184-10PAK
Indium tin oxide coated glass slide	70-100 Ω/sq	703176-10PAK
Indium tin oxide coated aluminosilicate glass slide	5-15 Ω/sq	576360-10PAK 576360-25PAK
Indium tin oxide coated glass slide	8-12 Ω/sq	578274-10PAK 578274-25PAK
Indium tin oxide coated glass slide	15-25 Ω/sq	636916-10PAK 636916-25PAK
Indium tin oxide coated glass slide	30-60 Ω/sq	636908-10PAK 636908-25PAK
Indium tin oxide coated glass slide	70-100 Ω/sq	576352-10PAK 576352-25PAK
Indium oxide coated PET	≤10 Ω/sq	700177-5PAK 700177-10PAK
Indium oxide coated PET	60-100 Ω/sq	702811-5PAK 702811-10PAK
Indium tin oxide coated PET	35 Ω/sq	639311-1EA 639311-5EA
Indium tin oxide coated PET	45 Ω/sq	668559-1EA 668559-5EA
Indium tin oxide coated PET	60 Ω/sq	639303-1EA 639303-5EA
Indium tin oxide coated PET	100 Ω/sq	639281-1EA 639281-5EA

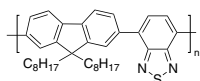
Indium Tin Oxide/Indium Oxide Powders

Name	Particle Size	Description	Cat. No.
Indium(III) oxide	particle size <100 nm (BET)	99.9% trace metals basis	632317-5G 632317-25G
Indium tin oxide	-325 mesh	99.99+% trace metals basis	494682-25G 494682-100G
Indium tin oxide	particle size <50 nm	-	544876-5G 544876-25G
Indium tin oxide, dispersion	particle size <100 nm (DLS)	30 wt. % in isopropanol	700460-25G 700460-100G

Light-Emitting Polymers



F8T2 (Aldrich Prod. No. 685070)
λ_{em} 497 nm in chloroform



F8BT (Aldrich Prod. No. 698687)
λ_{em} 515-535 nm in chloroform

Sigma-Aldrich® offers a wide variety of products for use in organic light-emitting diodes. Our product offerings include, but are not limited to:

- Electron Transport Materials
- Hole Transport Materials
- Hole Injection Materials
- Light-Emitting Polymers
- Polymer Hole and Transport Materials

Make Sigma-Aldrich Materials Science your one-stop source for organic electronic materials. Visit sigma-aldrich.com/oel for a full listing of products and literature pertaining to this field of study.

sigma-aldrich.com

SIGMA-ALDRICH®

Ruthenium-Based Dyes for Dye Solar Cells



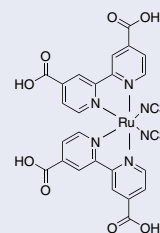
Dye solar cells (DSCs) are third generation solar cells with the promise of high efficiency combined with low production costs. While present day DSCs provide light-to-electricity conversion of up to 11%, significant further improvement is envisaged through optimized materials and novel cell and module architectures.

In dye sensitized solar cells, the dye is one of the key components for high-power conversion efficiencies. In recent years, considerable developments have been made in the engineering of the dye structure to enhance the performance of the system.

Particularly interesting are the amphiphilic homologues of the pioneering ruthenium based N-3 dye, for example, Z-907 (**Aldrich Prod. No. 703168**). The amphiphilic dyes display several advantages over the N-3 dye:

- 1) a higher ground state pK_a of the binding moiety thus increasing electrostatic binding onto the TiO_2 surface at lower pH values
- 2) decreased charge on the dye, attenuating electrostatic repulsion between adsorbed dye units and thereby increasing dye loading
- 3) increased stability of solar cells towards water-induced dye desorption
- 4) oxidation potential of these complexes is cathodically shifted compared to that of the N-3 sensitizer, which increases the reversibility of the ruthenium III/II couple, leading to enhanced stability.

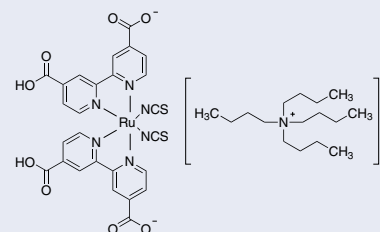
Ruthenium Dyes



Aldrich Prod. No. 703206

N-3: Basic dye for use in DSC. It efficiently sensitizes wide band gap oxide semiconductors such as titanium oxide up to wavelengths of 700nm.

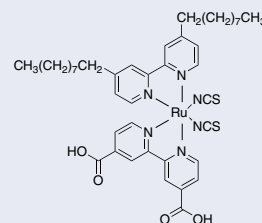
Molecular Formula: $C_{26}H_{16}N_6O_8RuS_2$,
Formula Weight: 705.64



Aldrich Prod. No. 703214

N-719 dye: Modification of N-3 to increase cell voltage and is the most common high performance dye.

Molecular Formula: $C_{58}H_{86}N_8O_8RuS_2$,
Formula Weight: 1188.55



Aldrich Prod. No. 703168

Z-907 dyes: Hydrophobic dye, very efficiently sensitizes wide band-gap titanium oxide up to 750 nm.

Molecular Formula: $C_{42}H_{52}N_6O_4RuS_2$,
Formula Weight: 870.10

U.S. Department of Energy's Materials Research for Advanced Lithium Ion Batteries



David Howell^{1*}, Tien Duong¹, John B. Deppe², Irwin Weinstock³

¹U.S. Department of Energy, Vehicle Technologies Program,
1000 Independence Avenue

Washington DC 20585

²Deppe Consulting, Washington D.C., 20585

³Sentech, Inc. 7475 Wisconsin Ave., Suite 900,
Bethesda, MD 20814

* E-mail: David.Howell@ee.doe.gov

Introduction

Increasing fuel costs and concerns about greenhouse gas emissions have spurred the growth in sales of hybrid electric vehicles (HEVs) that carry a battery pack to supplement the performance of the internal combustion engine (ICE). The next generation of hybrid electric vehicles, plug-in hybrid electric vehicles (PHEVs), will have the ability to recharge their energy storage system with electricity from a standard electric outlet. The key advantage of PHEVs is that they can use this stored electrical energy to propel the vehicle, meeting between 10 and 40 miles of urban driving needs with virtually no gasoline use, thus reducing petroleum consumption by the combustion engine. However, batteries used in today's power-assist HEVs do not have sufficient energy storage capability to meet the requirements of these advanced vehicles. The DOE, in partnership with the U.S. Advanced Battery Consortium (USABC, a partnership involving the three major domestic automakers formed to develop electrochemical energy storage technologies for fuel cell, hybrid, and electric vehicles), has been developing lithium rechargeable battery technology for several years. These efforts have resulted in significant improvements in the performance, life, and abuse resistance of batteries for vehicle applications.

Development Goals and Approach

The DOE, through its national laboratories has conducted vehicle analyses and battery sizing studies to recommend battery performance requirements for use by the USABC when soliciting proposals from potential battery developers and for benchmarking progress in the various development programs.¹ These analyses have shown that the energy storage requirements for PHEVs depend on the vehicle platform, vehicle performance on various drive cycles, hybrid configuration, operating strategy, and all-electric range capability, i.e., the total miles that can be driven using the stored energy. Battery performance requirements for vehicles with an all-electric range of 10 and 40 miles (PHEV 10 and PHEV 40) are summarized in **Table 1**.

Table 1. Battery power and energy requirements (at 30°C) for PHEV 10 and PHEV 40

Characteristics at EOL (End of Life)		2012 Targets	2016 Targets
All Electric range	miles	10	40
Peak Pulse Discharge Power—2 seconds	kW	50	46
Peak Pulse Discharge Power—10 seconds	kW	45	38
Peak Regen Pulse Power—10 seconds	kW	30	25
Available Energy @ 10 kW for Charge Depleting Mode	kWh	3.4	11.6
Maximum System Weight	kg	60	120
Maximum System Volume	liter	40	80
System Recharge Rate at 30°C, 120V	kW	1.4	1.4
Life	Deep Cycles ^a	3,000-5,000	
Life	Years	10-15	

(a) 70–80% depth-of-discharge

Vehicle-related battery research in the DOE is managed by the Electrochemical Energy Storage effort within the DOE's Vehicle Technologies Program (VT). This comprehensive R&D effort is composed of three major activities: *Battery Technology Development*, conducted in cooperation with the USABC, that sponsors cost-shared efforts with battery makers to develop and evaluate advanced lithium battery technologies for advanced vehicles; *Applied Battery Research*, in which six of DOE's national laboratories bring their own expertise to resolve the critical barrier areas of battery life, abuse tolerance, low temperature performance, and cost; and, *Long-term Battery Research*, conducted at national laboratories, universities, and battery materials developers, provides a better understanding of why systems fail, develops models that predict system failure and permit system optimization, and investigates new and promising materials.

The major goal of the materials-related research is to develop cell materials with increased energy density. Such new materials would result in batteries with fewer cells, less active and supportive materials, less cell and battery hardware, lower weight, lower volume, and, of course, reduced cost. **Figure 1** shows the progression from today's Li-ion chemistries to those that are being developed in the Energy Storage Program for future generations of PHEVs. These activities are described in the following sections.

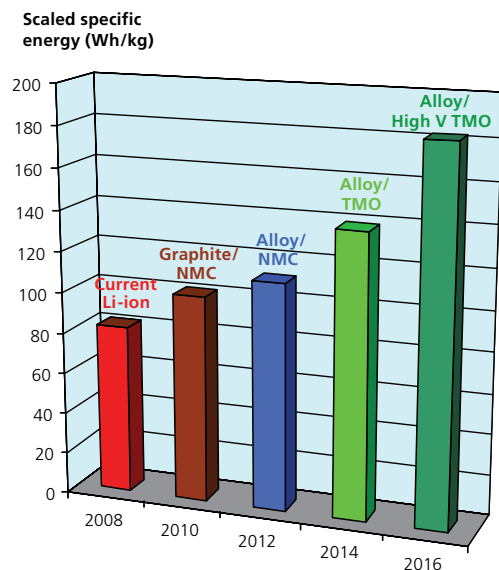


Figure 1. Energy gains from materials research

Materials Research

Background

Lithium metal is an attractive material for batteries due to its lightweight, high voltage, high electrochemical capacity per unit weight, and good conductivity (**Aldrich Prod. Nos. 220914, 62360, 62361**). Development of high-energy primary (non-rechargeable) batteries using lithium anodes started in the 1960's and these batteries were first used in the 1970's for military applications. Today these batteries are used in a variety of applications, including calculators, watches, cameras, memory backup circuits, etc.

Development of rechargeable batteries with lithium metal anodes started in the early 1980's. A number of rechargeable battery chemistries were developed, but due to persistent life and safety problems none achieved commercial success. These problems arise from lithium's reactivity with the electrolyte and its tendency to form mossy and sometimes dendritic deposits when recharged. These deposits lead to cell failures when the dendrites penetrate the separator and cause internal short circuits.

These problems were circumvented with the introduction of lithium-ion batteries (sometimes abbreviated Li-ion) in the early 1990's. These batteries contain no metallic lithium but instead rely on the transfer of lithium ions between the anode (negative electrode) and cathode (positive electrode), as illustrated in **Figure 2**. When the cell is charged, lithium ions are inserted or intercalated into the interstitial space between the atomic layers of the anode and during discharge the lithium is extracted from the anode and inserted into the cathode.² The lithium ions are transported between the electrodes in an electrolyte comprised of a lithium salt dissolved in an aprotic organic solvent. A typical electrolyte, widely used in the DOE programs, consists of LiPF_6 (**Aldrich Prod. No. 450227**) dissolved in a mixture of ethylene carbonate (EC, **Aldrich Prod. No. 676802**) and ethyl methyl carbonate (EMC). A separator layer, usually a microporous polyolefin film, such as Celgard® 2500, a 25 μm polypropylene membrane, is placed between the electrodes to prevent electrical shorts while allowing flow of ionic current.

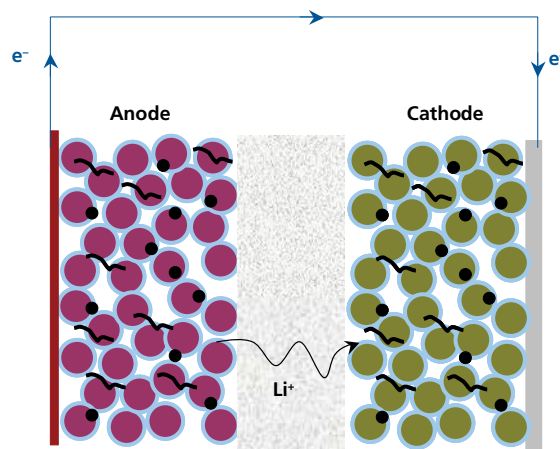


Figure 2. Schematic showing operation of Li ion cell

Anodes

The most popular material used as a host for lithium in the anode is graphitic carbon, usually supported on a copper substrate current collector. Other carbons, including both soft and hard carbons, have been used but graphitic carbons offer the best balance of reversible capacity and cycle life. When fully charged, all carbon materials approach to within 50 mV of the reversible lithium potential.

As an alternative to graphite, the DOE is investigating lithium alloys, including Li-Si, Li-Sn, and Li-Sb systems, and intermetallic electrodes, such as Cu_3Sn , Cu_6Sn_6 , and CoCu_5Sn_5 . These materials can provide an electrochemical potential only a few hundred mV above that of metallic lithium and a capacity of at least 400 mAh/g (>1500 mAh/ml).³ Alloys of lithium with metals and/or intermetallic compounds, however, experience severe volume expansion/contraction during the charging (alloying), and discharging (de-alloying) processes. When used in electrodes in Li-ion cells, these large volume changes lead to mechanical pulverization, loss of electronic contact between particles, and poor cycling. Approaches to alleviating this problem include using nanosized particles and/or including the alloying metal particles in a matrix phase to buffer the volume changes. These approaches are showing some improvements in experimental cells.

Metal oxides, such as lithium titanate (**Aldrich Prod. No. 400939**), that were previously investigated as positive electrode materials, have recently attracted attention as negative electrodes. The DOE program has studied the electrochemical and thermal properties of the $\text{Li}_4\text{Ti}_5\text{O}_{12}$ spinel⁴ and is now focused on LiTiO_2 . These materials generally have high reversible capacity (up to 600 mAh/g) and high lithium diffusion rates, though their potential against lithium is in the order of 1.0-1.5V. This results in a reduction of cell voltage and energy compared to cells using a carbonaceous anode with the same cathode and electrolyte. Moreover, these materials are extremely stable and can lead to battery systems that are inherently reliable and safe compared to other Li-Ion battery technologies. A new stable, nano-phase form of lithium titanate was developed that can provide an increase in the energy density of the cell and allow for easier industrial processing.

Cathodes

The majority of Li-ion batteries on the market today utilize lithium cobalt oxide (LiCoO₂, **Aldrich Prod. No. 442704**) as the positive electrode material. LiCoO₂ offers good electrical performance, is easily prepared, and is relatively insensitive to process variations and moisture. It may not, however, have the balance of properties needed to meet the stringent life, abuse tolerance, and cost targets of vehicle applications. As a consequence, DOE is evaluating several candidate lithiated metal oxide cathode materials that offer improvements over LiCoO₂.

Manganese oxides are inexpensive, environmentally benign, have excellent safety characteristics, and inherently high rate capability making them ideal candidates for advanced cathodes. Work is underway to improve the performance of Mn-based electrodes by developing a firm scientific understanding of the factors that control or influence electrochemical performance and utilize this to design and develop improved compositions. One approach being taken is cationic and anionic substitutions, e.g., substituting Li, Ni and/or Co for Mn and F for O. For example, a substituted spinel, LiMn_{1.8}Li_{0.1}Ni_{0.1}O_{3.8}F_{0.2}, exhibited improved electrochemical performance compared to a conventional LiMn₂O₄ cathode (**Aldrich Prod. No. 482277**). Another approach is the development of high-voltage, high-capacity electrodes with two-component integrated structures, e.g., 'layered-layered' xLi₂M'O₃•(1-x)LiMO₂ and 'layered-spinel' xLi₂M'O₃•(1-x)LiM₂O₄ electrodes in which M' is predominantly Mn and M is selected mainly from Mn, Ni and Co. In these composite structures, one layer is electrochemically active while the other is an electrochemically inactive, stabilizing component.

DOE is also investigating ways to improve the performance of LiFePO₄ cathodes. This effort is focused on developing composite cathodes with electrochemically-active polymers. The purpose is to replace electrochemically inactive cathode components, such as binders and conductive carbons, with electroactive materials that will contribute to the cell's energy storage capacity. The investigations include fabricating and evaluating carbon-coated LiFePO₄/polymer composite cathodes with polypyrrole (PPy, polymerized from a pyrrole monomer with sodium *p*-toluenesulfonate dopant and (NH₄)₂S₂O₈ (**Aldrich Prod. No. 215589**) as oxidizer in deionized water), polyaniline (PAN, synthesized from aniline with (NH₄)₂S₂O₈ as oxidizer in water), and polytriphenylamine (PTPA, obtained by polymerization of triphenylamine monomer with FeCl₃ (**Aldrich Prod. No. 236489**) as oxidizer in CHCl₃ solution). Different methods are being used to make these composite cathodes, including direct mixing of LiFePO₄ with the polymer and simultaneous chemical polymerization of PPy or PAN with LiFePO₄ in the precursor solution.

Electrolytes and the Solid Electrolyte Interphase (SEI)

Most practical electrolyte solvents are not thermodynamically stable at the low voltage of the negative electrode and a layer of decomposition products form spontaneously on the carbonaceous anode electrode surface during the first charge. This *solid electrolyte interphase (SEI)* layer protects the electrolyte from further decomposition while being ionically conductive and allowing passage of Li⁺ ions and is the key to stable battery performance. The dominant species in the SEI layer have been identified as lithium alkyl carbonates (ROCO₂Li) and lithium alkoxides (ROLi), and include Li oxalate, Li ethylene carbonate, and Li ethylene dicarbonate. Additional studies into the characteristics of the SEI layer and how they are impacted by cell fabrication and formation conditions are underway.

Research is also underway to understand the fundamental characteristics of Li⁺ transport to enable higher rate, more stable electrodes and electrolytes to be developed. First principles quantum chemistry calculations are being used to develop atomic force fields, which are then used in molecular dynamics simulations to investigate charge transport, bulk, and interfacial resistance. Among other findings, it has been discovered that the predicted charge transfer resistance increased over one order of magnitude when the temperature was decreased from room temperature to below 0°C, as observed experimentally, and that the main contribution to this increased resistance is the mean free energy associated with Li⁺ desolvation.

Research is also continuing to find an electrolyte that will permit the use of lithium metal as an anode since it offers the highest theoretical energy density of any known form of lithium. One approach being investigated is the development of a composite polymer electrolyte (with a hard non-conducting part that inhibits dendrites and second highly conducting portion) that mitigates the threat of dendritic growths that can short the cell. This concept, illustrated in **Figure 3**, holds the promise of enabling lithium rechargeable cells with two to three times the energy density of current lithium ion cells.

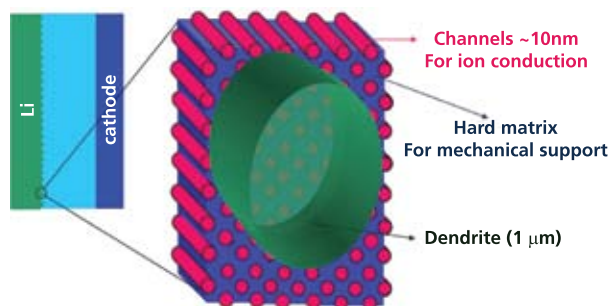


Figure 3. Schematic of composite electrolyte

Summary

The materials research and development activities described above are part of a comprehensive DOE effort to develop the advanced batteries needed to commercialize plug-in hybrid electric vehicles. The objective of this research is to give battery developers a range of materials for anodes, cathodes, and electrolytes that they might choose to incorporate in the cells and batteries that they are developing. The current battery development efforts, sponsored by DOE in partnership with the USABC, consist of four contracts to address critical issues of PHEV battery cost and life and incorporate many of the materials and technologies described above. This wide range of technologies is being explored in order to reduce the uncertainty of whether cost-competitive batteries with adequate performance and life can be commercialized by 2016.

References:

- (1) Ahmad A. Pesaran, et al, "Battery Requirements for Plug-In Hybrid Electric Vehicles - Analysis and Rationale," Electric Vehicle Symposium 23, Anaheim CA., December 2-5, **2007**.
- (2) Linden, David and Thomas B. Reddy, *Handbook of Batteries, Third Edition*, McGraw Hill, New York, **2002**.
- (3) *FY2007 Annual Progress Report for the DOE Energy Storage Research and Development Program*, January **2008**, available at http://www1.eere.energy.gov/vehiclesandfuels/resources/fcvt_reports.html.
- (4) *FY2005 Annual Progress Report for the DOE Energy Storage Research and Development Program*, January **2006**, available at http://www1.eere.energy.gov/vehiclesandfuels/resources/fcvt_reports.html

Select Materials for Battery Applications

For a complete list of battery related materials please visit sigma-aldrich.com/energy.

Electrode Materials

Name	Description	Cat. No.
Graphite, flakes	-	332461-2.5KG 332461-12KG
Graphite	O.D. x I.D. x L 80-200 nm x 0.5-10 nm x 0.5-20 μm	636398-2G 636398-10G 636398-50G
Graphite, rod	99.999%, L 150 mm diam. 6 mm	496553-180.7G
	99.999% trace metals basis, L 150 mm diam. 3 mm	496537-43.5G
Graphite, powder	99.99+% trace metals basis	496588-113.4G
	99.99+%	496596-113.4G
Graphite	99%, W x L 50-250 nm x 0.5-5 μm	698830-1G
Lithium, granular	≥99%	62360-10G-F 62360-50G-F
Lithium, wire	99%, diam. 3 mm	62358-50G-F
Lithium, granular	99.9+%, metals basis	499811-25G 499811-100G
Lithium, ingot	99.9% trace metals basis, diam. 5.7 cm	265977-115G 265977-460G
Lithium, ribbon	99.9% trace metals basis, thickness x W 1.5 x 100 mm	266000-25G 266000-100G
	99.9% trace metals basis, thickness x W 0.75 x 45 mm	265993-25G 265993-100G
	99.9% trace metals basis, thickness x W 0.75 x 19 mm	320080-25G 320080-100G
	99.9% trace metals basis, thickness x W 0.38 x 23 mm	265985-25G 265985-100G
Lithium, rod	99.9% trace metals basis, diam. 12.7 mm	265969-50G 265969-250G
Lithium, wire (in mineral oil)	99.9% trace metals basis, diam. 3.2 mm	220914-25G 220914-100G
Lithium cobalt(III) oxide	99.8% trace metals basis	442704-25G-A 442704-100G-A
Lithium iron(III) oxide	95%	442712-100G-A
Lithium manganese(III,IV) oxide	-	482277-25G
Lithium molybdate	99.9% trace metals basis	400904-50G 400904-250G
Lithium titanate	-	400939-100G 400939-500G
Manganese(II,III) oxide, powder	97%	377473-100G 377473-500G
Manganese(II) oxide, powder and chunks	99.99+% trace metals basis	431761-1G 431761-10G
Manganese(II) oxide, powder	99%	377201-500G
Manganese(IV) oxide, powder and chunks	99.99+%	529664-5G 529664-25G
Manganese(IV) oxide, solid	99.99% trace metals basis	203750-5G 203750-25G
Manganese(IV) oxide	≥99%	243442-5G 243442-100G 243442-500G

Electrolyte Materials

Name	Formula	Form	Purity	Cat. No.
Lithium hexafluoroarsenate(V)	LiAsF ₆	-	98%	308315-10G
Lithium hexafluorophosphate	LiPF ₆	powder	≥99.99% trace metals basis, battery grade	450227-5G 450227-25G
		powder	98%	201146-5G 201146-25G 201146-100G
	LiClO ₄	granular	99.99% trace metals basis	431567-50G 431567-250G
Lithium perchlorate	LiClO ₄	powder and chunks	99.99% trace metals basis	634565-10G 634565-100G
		granular	≥95.0%, ACS reagent	205281-5G 205281-100G 205281-500G
	-	beads	99.99% trace metals basis, anhydrous	451142-5G
Lithium tetrafluoroborate	LiBF ₄	powder	99.998% trace metals basis, anhydrous	451622-5G 451622-25G
		powder	98%	244767-10G 244767-50G
	LiBF ₄	liquid, 1.0 M in acetonitrile	-	255815-100ML

New Aldrich Handbook!

Over 6,000 innovative new products

Reserve your copy of the NEW 2009-2010 Aldrich set today.

2009-2010 Aldrich Handbook

- 10,000 chemical structures
- 8,500 updated literature citations
- Extensive chemical & physical data

Labware Catalog

- Innovative new products
- Improved product images
- New technical information index

Accelerating Customers' Success through Leadership in Life Science, High Technology and Service

ALDRICH
Chemistry

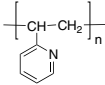


To request your complimentary
Aldrich Handbook set, visit
sigma-aldrich.com/aldrichcat

sigma-aldrich.com

SIGMA-ALDRICH

Solvents

Name	Structure	Description	Cat. No.
γ-Butyrolactone		≥99%, GC	H7629-500G H7629-1KG
		≥99%	B103608-25G B103608-500G B103608-3KG B103608-20KG
1,2-Dimethoxyethane	<chem>H3COCH2CH2OCH3</chem>	99.9%	307432-100ML 307432-1L 307432-2L
		≥99%	256382-1L 256382-2L
		≥99.5%, GC	38569-500ML-F 38569-1L-F
1,3-Dioxolane		99.8%	271020-100ML 271020-1L 271020-2L
		99%	184497-500ML 184497-1L 184497-4L
Poly(2-vinylpyridine)		M _n ~6100 M _p ~6400 M _w ~6500	81624-100MG
		M _n ~19900 M _p ~20900 M _w ~20500	81628-100MG
		M _n ~75500 M _p ~79500 M _w ~79100	81635-100MG
		average M _n 4,800 (Typical) average M _w 5,000 (Typical)	523291-1G
		average M _n 9,500 (Typical) average M _w 11,000 (Typical)	523305-1G
		average M _n 35,000 (Typical) average M _w 37,500 (Typical)	523321-1G
		average M _n 78,500 (Typical) average M _w 121,500 (Typical)	523348-1G
average M _n 152,000 (Typical) average M _w 159,000 (Typical)	523356-1G		
Propylene carbonate		99.7%	310328-100ML 310328-500ML 310328-1L 310328-2L
		99.7%	414220-1L 414220-2L
Thionyl chloride		99.5%	447285-5ML 447285-100ML 447285-500ML
		≥99%	230464-5ML 230464-100ML 230464-1L
		≥99%	320544-1L 320544-2.5L

Argentina

SIGMA-ALDRICH DE ARGENTINA S.A.
Free Tel: 0810 888 7446
Tel: (+54) 11 4556 1472
Fax: (+54) 11 4552 1698

Australia

SIGMA-ALDRICH PTY LTD.
Free Tel: 1800 800 097
Free Fax: 1800 800 096
Tel: (+61) 2 9841 0555
Fax: (+61) 2 9841 0500

Austria

SIGMA-ALDRICH HANDELS GmbH
Tel: (+43) 1 605 81 10
Fax: (+43) 1 605 81 20

Belgium

SIGMA-ALDRICH NV/S.A.
Free Tel: 0800 14747
Free Fax: 0800 14745
Tel: (+32) 3 899 13 01
Fax: (+32) 3 899 13 11

Brazil

SIGMA-ALDRICH BRASIL LTDA.
Free Tel: 0800 701 7425
Tel: (+55) 11 3732 3100
Fax: (+55) 11 5522 9895

Canada

SIGMA-ALDRICH CANADA LTD.
Free Tel: 1800 565 1400
Free Fax: 1800 265 3858
Tel: (+1) 905 829 9500
Fax: (+1) 905 829 9292

China

SIGMA-ALDRICH (SHANGHAI)
TRADING CO. LTD.
Free Tel: 800 819 3336
Tel: (+86) 21 6141 5566
Fax: (+86) 21 6141 5567

Czech Republic

SIGMA-ALDRICH spol. s r. o.
Tel: (+420) 246 003 200
Fax: (+420) 246 003 291

Denmark

SIGMA-ALDRICH DENMARK A/S
Tel: (+45) 43 56 59 10
Fax: (+45) 43 56 59 05

Finland

SIGMA-ALDRICH FINLAND OY
Tel: (+358) 9 350 9250
Fax: (+358) 9 350 92555

France

SIGMA-ALDRICH CHIMIE S.à.r.l.
Free Tel: 0800 211 408
Free Fax: 0800 031 052
Tel: (+33) 474 82 28 00
Fax: (+33) 474 95 68 08

Germany

SIGMA-ALDRICH CHEMIE GmbH
Free Tel: 0800 51 55 000
Free Fax: 0800 64 90 000
Tel: (+49) 89 6513 0
Fax: (+49) 89 6513 1160

Greece

SIGMA-ALDRICH (O.M.) LTD.
Tel: (+30) 210 994 8010
Fax: (+30) 210 994 3831

Hungary

SIGMA-ALDRICH Kft
Ingyenes telefonszám: 06 80 355 355
Ingyenes fax szám: 06 80 344 344
Tel: (+36) 1 235 9055
Fax: (+36) 1 235 9050

India

SIGMA-ALDRICH CHEMICALS
PRIVATE LIMITED
Telephone
Bangalore: (+91) 80 6621 9600
New Delhi: (+91) 11 4358 8000
Mumbai: (+91) 22 2570 2364
Hyderabad: (+91) 40 4015 5488
Fax
Bangalore: (+91) 80 6621 9650
New Delhi: (+91) 11 4358 8001
Mumbai: (+91) 22 2579 7589
Hyderabad: (+91) 40 4015 5466

Ireland

SIGMA-ALDRICH IRELAND LTD.
Free Tel: 1800 200 888
Free Fax: 1800 600 222
Tel: +353 (0) 402 20370
Fax: +353 (0) 402 20375

Israel

SIGMA-ALDRICH ISRAEL LTD.
Free Tel: 1 800 70 2222
Tel: (+972) 8 948 4100
Fax: (+972) 8 948 4200

Italy

SIGMA-ALDRICH S.r.l.
Numero Verde: 800 827018
Tel: (+39) 02 3341 7310
Fax: (+39) 02 3801 0737

Japan

SIGMA-ALDRICH JAPAN K.K.
Tel: (+81) 3 5796 7300
Fax: (+81) 3 5796 7315

Korea

SIGMA-ALDRICH KOREA
Free Tel: (+82) 80 023 7111
Free Fax: (+82) 80 023 8111
Tel: (+82) 31 329 9000
Fax: (+82) 31 329 9090

Malaysia

SIGMA-ALDRICH (M) SDN. BHD
Tel: (+60) 3 5635 3321
Fax: (+60) 3 5635 4116

Mexico

SIGMA-ALDRICH QUÍMICA, S.A. de C.V.
Free Tel: 01 800 007 5300
Free Fax: 01 800 712 9920
Tel: 52 722 276 1600
Fax: 52 722 276 1601

The Netherlands

SIGMA-ALDRICH CHEMIE BV
Free Tel: 0800 022 9088
Free Fax: 0800 022 9089
Tel: (+31) 78 620 5411
Fax: (+31) 78 620 5421

New Zealand

SIGMA-ALDRICH NEW ZEALAND LTD.
Free Tel: 0800 936 666
Free Fax: 0800 937 777
Tel: (+61) 2 9841 0555
Fax: (+61) 2 9841 0500

Norway

SIGMA-ALDRICH NORWAY AS
Tel: (+47) 23 17 60 60
Fax: (+47) 23 17 60 50

Poland

SIGMA-ALDRICH Sp. z o.o.
Tel: (+48) 61 829 01 00
Fax: (+48) 61 829 01 20

Portugal

SIGMA-ALDRICH QUÍMICA, S.A.
Free Tel: 800 202 180
Free Fax: 800 202 178
Tel: (+351) 21 924 2555
Fax: (+351) 21 924 2610

Russia

SIGMA-ALDRICH RUS, LLC
Tel: +7 (495) 621 6037
+7 (495) 621 5828
Fax: +7 (495) 621 5923

Singapore

SIGMA-ALDRICH PTE. LTD.
Tel: (+65) 6779 1200
Fax: (+65) 6779 1822

Slovakia

SIGMA-ALDRICH spol. s r. o.
Tel: (+421) 255 571 562
Fax: (+421) 255 571 564

South Africa

SIGMA-ALDRICH
SOUTH AFRICA (PTY) LTD.
Free Tel: 0800 1100 75
Free Fax: 0800 1100 79
Tel: (+27) 11 979 1188
Fax: (+27) 11 979 1119

Spain

SIGMA-ALDRICH QUÍMICA, S.A.
Free Tel: 900 101 376
Free Fax: 900 102 028
Tel: (+34) 91 661 99 77
Fax: (+34) 91 661 96 42

Sweden

SIGMA-ALDRICH SWEDEN AB
Tel: (+46) 8 742 4200
Fax: (+46) 8 742 4243

Switzerland

SIGMA-ALDRICH CHEMIE GmbH
Free Tel: 0800 80 00 80
Free Fax: 0800 80 00 81
Tel: (+41) 81 755 2828
Fax: (+41) 81 755 2815

United Kingdom

SIGMA-ALDRICH COMPANY LTD.
Free Tel: 0800 717 181
Free Fax: 0800 378 785
Tel: (+44) 1747 833 000
Fax: (+44) 1747 833 313
SAFC (UK) Tel: 01202 712305

United States

SIGMA-ALDRICH
P.O. Box 14508
St. Louis, Missouri 63178
Toll-Free: 800 325 3010
Toll-Free Fax: 800 325 5052
Call Collect: (+1) 314 771 5750
Tel: (+1) 314 771 5765
Fax: (+1) 314 771 5757

Internet

sigma-aldrich.com



Mixed Sources

Product group from well-managed
forests, controlled sources and
recycled wood or fiber
www.fsc.org Cert no. SGS-COC-003338
© 1996 Forest Stewardship Council



World Headquarters

3050 Spruce St., St. Louis, MO 63103
(314) 771-5765
sigma-aldrich.com

Order/Customer Service (800) 325-3010 • Fax (800) 325-5052

Technical Service (800) 325-5832 • sigma-aldrich.com/techservice

Development/Bulk Manufacturing Inquiries SAFC™ (800) 244-1173

©2008 Sigma-Aldrich Co. All rights reserved. SIGMA, SAFC, SAFC™, SIGMA-ALDRICH, ALDRICH, FLUKA, and SUPELCO are trademarks belonging to Sigma-Aldrich Co. and its affiliate Sigma-Aldrich Biotechnology, L.P. Sigma brand products are sold through Sigma-Aldrich, Inc. Sigma-Aldrich, Inc. warrants that its products conform to the information contained in this and other Sigma-Aldrich publications. Purchaser must determine the suitability of the product(s) for their particular use. Additional terms and conditions may apply. Please see reverse side of the invoice or packing slip. Nafion is a registered trademark of E.I. du Pont de Nemours & Co., Inc. ESCAT is a trademark of Engelhard Corp. Eppendorf is a registered trademark of Eppendorf-Netheler-Hinz GmbH. Sepharose is a registered trademark of GE Healthcare. Coomassie is a registered trademark of Imperial Chemical Industries Ltd. Plexcore is a registered trademark of Plextronics, Inc. NanoThinks and ProteoSilver are trademarks of Sigma-Aldrich Biotechnology LP and Sigma-Aldrich Co. CHROMASOLV, Pure-Pac, ReagentPlus, and TraceSELECT are registered trademarks of Sigma-Aldrich Biotechnology LP and Sigma-Aldrich Co. Celgard is a registered trademark of Celgard LLC.

LBE
70798-503403
0118